

Responses to Reviewers' Comments

We would like to thank the reviewers for their valuable and positive feedback/comments, which helped us to improve the manuscript.

Referee comments are given in black, and our point-to-point responses are in green. Changes made to the manuscript are marked in underlined green. The line number referred here is for the new revised manuscript.

Anonymous Referee #1

This manuscript promotes two new approaches to analyze complex mass spectra (here of highly oxygenated molecules (HOM)) with the goal to extract as much as possible information from the whole mass spectroscopic information: binwise PMF and coordinated PMF analysis in selected mass ranges. The authors suggest to select certain mass ranges for analysis according to expected time scales of production processes and sink processes, whereby they have condensation loss as major sink in mind. The approach is exercised at an ambient data set, measured by NO₃-CI_APITOF in September 2016 at the SMEAR II station in Finland. The manuscript is very well written, it is informative and very interesting to read. It discusses the limits (and strengths) of PMF analysis of atmospheric observations in the context of the variability of production and sinks processes of gaseous compounds in the atmosphere. It also points out two new observations - day time dimers and night time dimer nitrates-, which need mechanistic explanations. The focus of the paper is on the methodology, although along its development it reveals insight into HOM formation processes. I suggest highlighting the latter already more in the Discussion sections and summarizing it again in Atmospheric Insights section. I also suggest shortening the Contaminant Factor section and place some text from here into the supplement. See also comments. In the larger parts I see the manuscript - even in its given form - as an original and important contribution of general interest to atmospheric scientists, as nowadays in many atmospheric fields research is based on high resolution mass spectrometry. I suggest publishing the manuscript in ACP after the authors have addressed the (minor) comments below.

Comments

Abstract, line 36: Don't present your new findings as appendix. "As two mayor insights of our analysis scheme, we identified daytime dimer formation. . . We separated dimer formation by NO₃ oxidation.... "

Response 1.1: We agree with the reviewer. We have revised this part from "In addition, daytime dimer formation (diurnal peak around noon) was identified, which may contribute to NPF in Hyytiälä. Also, dimers from NO₃ oxidation were separated by the sub-range binPMF, which would not be identified otherwise." to

"As two major insights from our study, we identified daytime dimer formation (diurnal peak around noon) which may contribute to NPF in Hyytiälä, as well as dimers from NO₃ oxidation process." in Line 36-38.

Introduction, line 87: Could the authors comment on the role of chemical losses compared to condensation losses onto particles. Couldn't chemical losses, e.g. by oxidation of HOM by OH, enhance the window of sink time scales?

Response 1.2: Both Peräkylä et al. (2020) and Bianchi et al. (2019) assess the impact of oxidation on the HOM lifetime, and find that it's negligible under typical conditions. Condensation dominates, even when assuming collision limited reaction with OH radicals. However, for compounds of higher volatility, such as IVOC and SVOC, oxidation could reduce their lifetime. We added the following explanation in Line 87:

“.....which may affect the factor analysis. For compounds of low volatility, such as many HOM, the main atmospheric loss process is typically condensation onto aerosol particles, with chemical sink being negligible (Bianchi et al., 2019). If, on the other hand, a compound does not irreversibly condense, oxidation reactions can also affect its lifetime.”

Introduction, line 93: Peräkylä et al., 2019 is not a suited reference for such a general statement.

Response 1.3: Ok, we removed this reference from here.

Introduction, line 121: The impact of the oxidants is different at different times of the day. That should limit important formation pathways to less than 6.

Response 1.4: We agree with the reviewer that different oxidants have their major impacts during different times of a day. Our initial goal here was just to point out there can be at most six pathways to form dimers, if considering the same precursor, formed from the same or different oxidants (O₃, OH, NO₃), so as to remind the readers that molecules from different ranges may have different formation pathways. To minimize the misunderstanding, we modified the sentence into

“..... RO₂+RO₂ reactions (Berndt et al., 2018a;Berndt et al., 2018b). This also means that there can be several different pathways to form dimers from the same precursor VOC, by combining RO₂ formed from the same or different oxidants. As an example of the latter” in Line 124.

Introduction, line 126: RO₂ + RO₂ also lead to monomer termination products. Thus, the statement is not valid in such generality. Maybe one should modify the sentence: . . .in monomer products (not terminated by RO₂), dependent on only one oxidant. . .

Response 1.5: For RO₂ + R'O₂ reactions, as reviewed by Orlando and Tyndall (2012) and (Bianchi et al., 2019), there are two main direct RO₂ termination reactions:



Reaction channel (a) will lead to monomer termination products, and (b) will lead to dimer products. It is true that RO₂ + RO₂ forms also monomer products. However, what we specifically meant, is that in this case, the formed monomer does not care about the identity of the other RO₂ taking part in the reaction, other than potentially about whether a carbonyl or an alcohol will be formed (Orlando and Tyndall, 2012). Thus, to a first approximation, in the RO₂+RO₂ terminated

monomer channel, any RO₂ will do as the terminator. This is in contrast with the dimer case, where the identity of both RO₂ will impact the formed dimer. To make it clear, we replaced the sentences in Line 128-133 “Such a molecule will not have a direct equivalent in any of the monomer products, dependent on only one oxidant, which again may complicate the separation of such factors by PMF, if the entire spectrum is analyzed once. However, if separating the monomer and dimer products before PMF analysis, separation of different formation pathways can potentially become simpler.”,

with “Such a molecule will not have a direct equivalent in any of the monomer products: even though monomers can form from RO₂ + R’O₂ reactions, the products from RO₂ are not dependent on the source of the R’O₂. This may complicate the identification of certain dimer factors by PMF if the entire spectrum is analyzed at once, and therefore separation of the monomer and dimer products before the PMF analysis could be advantageous.”

Introduction, line 145: It would be wishful to refer also already here to the new atmospheric information not only to “meaningful factors”. In the sense of “we will show that we were able to separate process x from process y”.

Response 1.6: We have revised this part in Line 145 from “..... run on the combined ranges. We found that more meaningful factors are separated from our dataset by utilizing the sub-ranges, and believe that this study will provide new perspectives for future studies” to

“..... run on the combined ranges. We found that dimers generated during daytime and dimers initiated by NO₃ oxidation can be separated from our dataset by utilizing the sub-ranges, but not with the full range. We believe that this study will provide new perspectives for future studies”

Result, line 295: This sentence is hard to understand, please, split and reformulate.

Response 1.7: To make it clearer, we have changed the sentence from “..... Factors 1-3 are all daytime factors, while Factor 4 has a sawtooth shape, which is caused by contamination, mainly by perfluorinated acids, of the inlet’s automated zeroing every three hours during the measurements (Zhang et al., 2019).” to

“..... Factors 1-3 are all daytime factors, while Factor 4 has no clear diurnal cycle, but a distinct sawtooth shape. Factor 4 comes from a contamination of perfluorinated acids, from the inlet’s automated zeroing every three hours (Zhang et al., 2019).” in Line 313-315.

Discussion, line 448: hard to understand and possibly a verb missing. Please, reformulate.

Response 1.8: To make it easier to understand, we have changed the sentence from “..... (R3F1_D) basically has no obvious markers in the profile, and as mentioned above, up to ten factors, there would only be more factors fragmented from the previous factor, with similar spectral profiles, but showed different profile pattern with 510 – 560 Th in RCF2_D2 in Range Combined. The factorization of Range Combined was mainly controlled by Range 1 and 2 due to high signals, and the signals in Range 3 are forced to be distributed according to the time series determined by Ranges 1 and 2. Ultimately, this will lead to” to

“..... (R3F1_D) has no obvious markers in the profile. With the increase of factor number (up to ten factors), no clearly new factors were separated in Range 3, but instead the previously

separated factors were seen to split into several factors. However, the spectral pattern in R3F1_D is different from that in the mass range of 510 – 560 Th in RCF2_D2. The factorization of Range Combined was mainly controlled by low masses due to their high signals. The signals at high masses were forced to be distributed according to the time series determined by small masses. Ultimately, this will lead to” in Line 476-482.

Discussion, line 468 and 474: Did you search for specific marker ions (odd mass) in the monomer range? Maybe, singular nitrates are formed quite efficiently and the corresponding nitrate peroxy radicals could be involved in the dimer formation. Could NO₃ radicals attack the dimers the dimer?

Response I.9: (1) As the reviewer suggests, the possible monomers initiated by NO₃ oxidation would have odd integer masses, as listed in Table R1.

Table R1 potential monomers initiated by NO₃ oxidation and their corresponding integer masses

Number of O atom (x)	C ₁₀ H ₁₅ NO _x NO ₃ ⁻	C ₁₀ H ₁₇ NO _x NO ₃ ⁻
1	227	229
2	243	245
3	259	261
4	275	277
5	291	293
6	307	309
7	323	325
8	339	341
9	355	357

In the monomer range (Range 2), the only night factor (as shown below in Figure R1) is R2F4_N. 325 Th is the highest odd mass in Range 2, with no other significant odd-mass markers. We can do a high-resolution fit to 325 Th, with center mass of 325.06 Th and resolution of 3577 Th/Th, which is quite close to the instrument resolution, ~4000 Th/Th. There can be mainly two candidates for 325 Th, the radical C₁₀H₁₅O₈NO₃⁻ (with exact mass of 325.0651 Th) and monomer from NO₃ oxidation C₁₀H₁₇NO₇NO₃⁻ (with exact mass of 325.0889 Th). In our case, this 325 Th is more likely the radical. In addition, R2F4_N shows significantly higher correlation with ozonolysis dimers (R3F2_N1) (R² = 0.75) compared to the NO₃ oxidation dimer (R3F3_N2) (R² = 0.27). A similar result is also found in the combined range, as shown in Figure R2. We thus conclude that any potential monomer nitrates are minor compared to the non-nitrate monomers, and an instrument with much higher resolution, e.g. the CI-Orbitrap (Riva et al., 2019), would be needed to unambiguously identify such compounds.

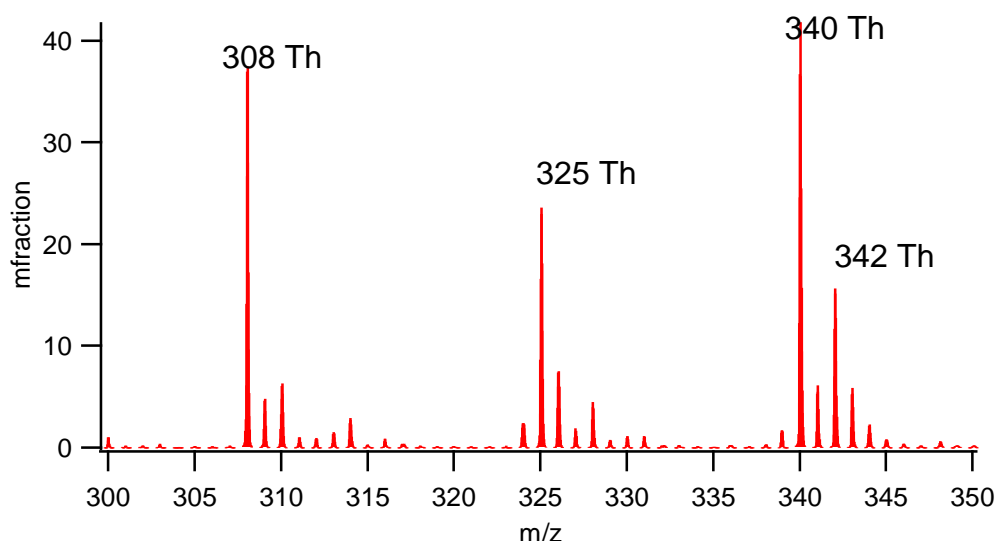


Figure R1 Spectral profile of R2F4_N in fraction, with the main m/z marked

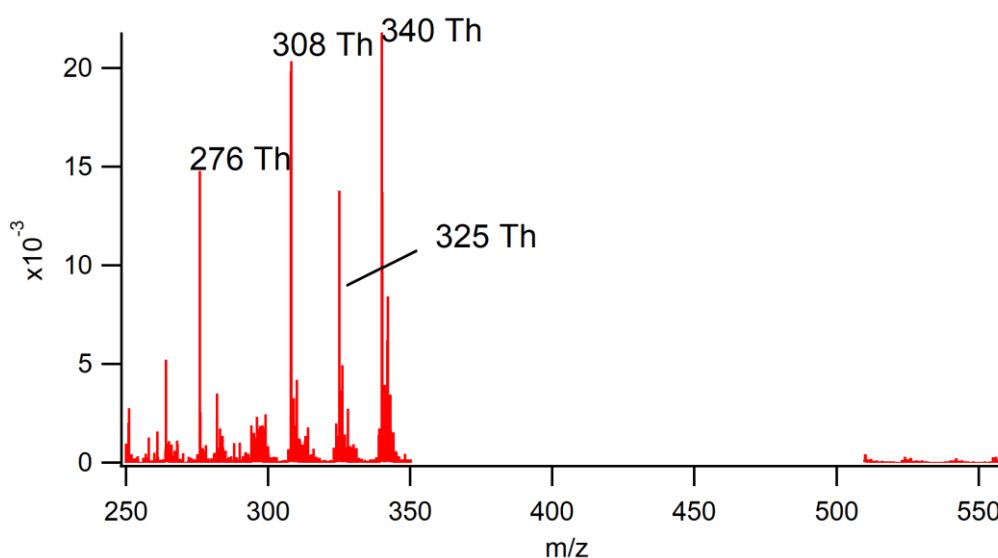


Figure R2 Spectral profile of RCF4_N in fraction, with the main m/z marked in the monomer range

The detection of nitrate dimers of course mean that NO₃-initiated radicals do form efficiently, and participate in the dimer formation by providing the RO₂ supply. We only argue that the potential to undergo autooxidation, and thus form HOM monomers, is limited for the monoterpenes during these measurements. As even less oxidized dimers condense very efficiently, they will have very limited (see also *Response 1.2*) time to react with NO₃ radicals, meaning that it's unlikely that the observed nitrate dimers would be formed from a reaction between nitrate radicals and non-nitrate dimers.

Discussion, line 485-548: I find that whole section too lengthy. I agree that the authors performed a smart analysis to find out why contamination factors do correlate or not. However, is this argumentation really needed to demonstrate that different loss rates lead to different time profiles, thus attribution to different factors, if the source is the same? Insofar I find the jump from the

contamination analysis to ambient data in line 541 somewhat disturbing. At least a new paragraph should start here. I suggest to place the text of contamination analysis in large parts into the supplement. In the manuscript I would just state that a detailed analysis explained why contamination factors do not correlate and refer to the supplement. The space saved could be used to more underline the atmospheric findings somewhat more (all over the manuscript and in the Atmospheric Insights section).

Response 1.10: We agree with the reviewer, and have moved most of the text of this part to supplement. Only the results, discussions of low correlations between different contamination compounds, and indications of volatility effect on factor analysis were kept.

Atmospheric Insights, line 550: “While the previous section discussed several findings with atmospheric implications,..” I suggest to sample and to discuss at this point the insights into the HOM formation processes mentioned in all the discussion sections. And maybe elaborate the two new findings somewhat more.

Response 1.11: Thanks for the comments. (1) For the “4. Discussion” part, we adjusted and revised the structure of this part, and rearranged and added the relative contents in different sections, respectively. The previous structure in the “4. Discussion” was:

“4. Discussion

4.1 Comparison of different ranges

4.1.1 Time series correlation

4.1.2 Daytime factor comparison

4.1.3 Nighttime factor comparison

4.1.4 Contamination factor

4.2 Atmospheric insights

4.2.1 Daytime dimer formation

4.2.2 Dimers initiated by NO₃ radicals”,

while the new adjusted structure is

“4. Discussion

4.1 Time series correlation

4.2 Daytime processes

4.2.1 Factor comparison

4.2.2 Daytime dimer formation

4.3 Nighttime processes

4.3.1 Factor comparison

4.3.2 Dimers initiated by NO₃ radicals

4.4 Fluorinated compounds

4.5 Atmospheric insights”.

(2) Now the section “4.5 Atmospheric insights” was simplified and mainly summarized the key atmospheric insights which have been discussed in more details in sections 4.1-4.3.

“Based on the new data analysis technique binPMF applied in sub-ranges of mass spectra, we were able to separate two particularly intriguing atmospheric processes, the formation of daytime

dimers as well as dimer formation involving NO_3 radicals, which otherwise could not have been identified in our study.

With a diurnal peak around noon time, the daytime dimers identified in this study correlate very well with daytime factors in monomer range. Strong correlation between this factor and solar radiation indicate the potential role of OH oxidation in the formation of daytime dimers. By now, very few studies have reported the observations of daytime dimers. As dimers are shown to be able to take part in new particle formation (NPF) (Kirkby et al., 2016), this daytime dimer may contribute to the early stages of NPF in the boreal forest.

The second process identified in our study is the formation of dimers that are a crossover between NO_3 and O_3 oxidation. Such dimers have been identified before (Yan et al., 2016). However, we were not able to identify corresponding HOM monomer compounds. This finding indicates that while NO_3 oxidation of the monoterpenes in Hyytiälä may not undergo autooxidation to form HOM by themselves, they can contribute to HOM dimers when the NO_3 -derived RO_2 react with highly oxygenated RO_2 from other oxidants. Multi-oxidant systems should be taken into consideration in future experimental studies on monoterpene oxidation processes.”

(3) To elaborate the results more, we also added more discussion by including NO_3 radical measurements in the same IBARN campaign by Liebmann et al. (2018), in section 4.3.2 in Line 548-572, as follows:

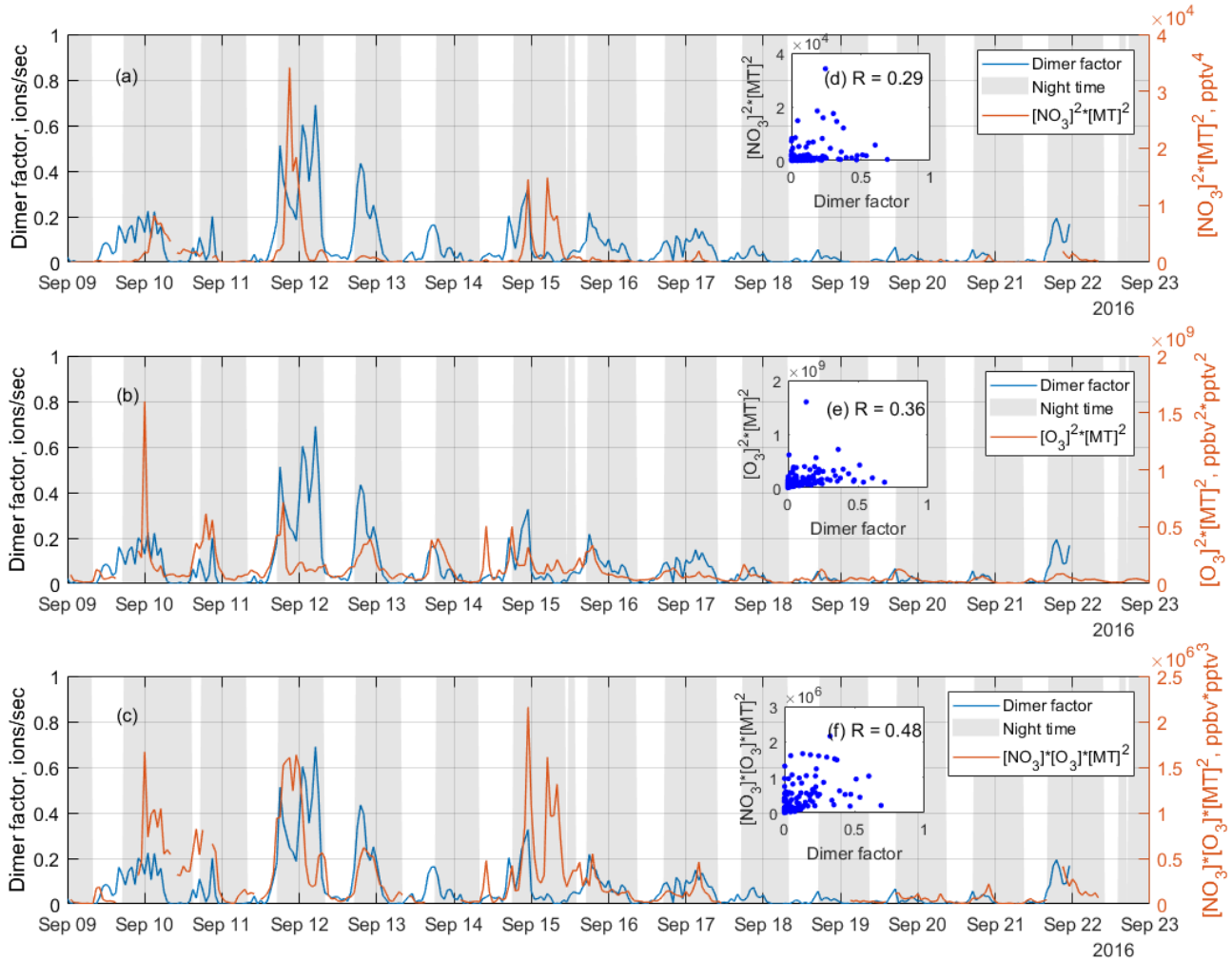


Figure R3 (Figure 7 in the manuscript) Time series of the NO₃ oxidation dimer factor (blue line), and the product of (a) [NO₃]² × [monoterpene]², (b) [O₃]² × [monoterpene]², and (c) [NO₃] × [O₃] × [monoterpene]², where [] represents concentration in unit of pptv for NO₃ radicals and monoterpene, ppbv for O₃, while the scatter plots are shown as inserts, (d), (e), (f), respectively. The scatter plots and correlation coefficients R are only calculated from nighttime data, which is selected based on solar radiation, to eliminate the influence from daytime oxidation processes.

“.....Thus, while there are to our knowledge no laboratory studies on HOM formation from NO₃ oxidation of α-pinene, a low yield can be expected based on SOA studies.

As discussed above, a dimer factor (R3F2 N2) was identified as being a crossover between NO₃ radical initiated and O₃ initiated RO₂ radicals. Figure 7 shows the time series of this factor, as well as the product of [NO₃]² × [monoterpene]², [O₃]² × [monoterpene]², and [NO₃] × [O₃] × [monoterpene]². These products are used to mimic the formation rates of the RO₂ radicals reacting to form the dimers, either from pure NO₃ oxidation (Fig. 7a), pure O₃ oxidation (7b), or the mixed reaction between RO₂ from the two oxidants (7c). The NO₃ concentration was estimated in Liebmann et al. (2018) for the same campaign. Monoterpenes were measured using a proton transfer reaction time of flight mass spectrometer (PTR-TOF-MS). More details on measurement of NO₃ proxy and monoterpene can be found in in Liebmann et al. (2018).

As shown in Figure 7, the time series of the dimer factor tracks those of [NO₃] × [monoterpene] and [O₃] × [monoterpene] reasonably well, but shows the highest correlation with the product of [NO₃] × [O₃] × [monoterpene]². This further supports this dimer formation as a mixed processes of ozonolysis and NO₃ oxidation. The heterogeneity of the monoterpene emissions in the forest, and the fact that no dimer loss process is included, partly explain the relatively low correlation coefficients. The sampling inlets for PTR-TOF were about 170 m away from the NO₃ reactivity measurement (Liebmann et al., 2018), which in turn was some tens of meters away from the HOM measurements. Thus, this analysis should be considered qualitative only.

The nitrate dimer factor (R3F2 N2) was dominated by the organonitrate at 555 Th, C₂₀H₃₁O₁₀NO₃·NO₃⁻. However, unlike the pure ozonolysis dimer factor which had a corresponding monomer factor”

Conclusion, line 633: As mentioned before, highlight the new atmospheric findings here. Prevent presenting it as an appendix to your methodological approach. Minor Figure captions are not separated well from running text.

Response 1.12: (1) For the conclusion, as both reviewer suggested, changes have been made to simplify the conclusion and highlight the new findings. The new revised conclusion is as follows:

“The recent development in mass spectrometry, combined with factor analysis such as PMF, has greatly improved our understanding of complicated atmospheric processes and sources. However, one of PMF’s basic assumptions is that factor profiles remain constant in time, yet for atmospheric gas-phase species, reactions and sinks may violate this assumption. In this study, we conducted separate binPMF analysis on three different sub-ranges to explore the potential benefits of such an approach for producing more physically meaningful factors.

With binPMF applied on sub-ranges, our study identified daytime dimers, presumably initiated by OH/O₃ with a diurnal peak at around noon, which may contribute to NPF in Hyytiälä. Also, based on the sub-range binPMF analysis, we successfully separated NO₃-related dimers which

did not have a corresponding monomer factor. The NO₃-related factor was consistent with earlier observations (Yan et al., 2016), but would not have been identified from this dataset without utilizing the different sub-ranges. In future laboratory experiments, more complex oxidation systems may be useful in order to understand the role of NO₃ oxidation in SOA formation. Apart from these two findings, we also find other benefits by applying binPMF on sub-ranges of the mass spectra.

First, volatility affects the PMF results. Different compounds emitted from the same source showed different temporal trends, likely due to differences in volatilities. This increased the difficulties for PMF to separate this source in the combined data set, and the resolved profile was less accurate than that of the sub-ranges. Future studies of gas-phase mass spectra should pay attention to this volatility effect on factor analysis.

Secondly, chemistry or sources contributing to the particular range can be better separated. Only the binPMF analysis on Range 3, where HOM dimers are typically observed, resolved two nighttime factors, characterized by monoterpene oxidation related to NO₃ and O₃ oxidation.

Thirdly, peaks with smaller signal intensities can be correctly assigned. The signal intensities between different parts of the mass spectrum may vary by orders of magnitude. In the combined case, the results were almost completely controlled by the higher signals from smaller masses. The separate analysis on Range 3 allowed the low signals to provide important information. In addition, running binPMF on different separate mass ranges also allows us to compare the factors obtained from the different ranges and help to verify the results.”

(2) Minor figure captions are modified into smaller font size, so as to be better separated from the main text.

line 119: any instead of many ?

Response 1.13: Yes, changed.

line 468: Please, replace “this factor” by the name of the factor “factor R2F4_N” for faster readability, because there was more than one factor listed in the previous sentence.

Response 1.14: Yes, changed.

Anonymous Referee #2

This manuscript presents binPFM (Positive matrix factorization) analysis results of subranges of mass spectra and combined ranges of mass spectra, respectively. The authors compared the results from three sub-ranges and the combined three, and concluded that the PFM results depended on the volatility of the species that is assumed to be identical among species, the chemistry or source that contributes to a particulate range of species, and the relative abundance of different species. The authors also discussed the potential formation mechanisms of observed species, especially dimers formed from peroxy radicals. Generally this is a very interesting study that clearly shows the potential issue when applying the PMF methods to measurements of volatile organic compound with different volatilities, which is of interest to the atmospheric chemistry community. On the other hand, the manuscript is a little bit too technical for Atmospheric chemistry and physics, but can be revised to

fit. I would recommend publication of this manuscript after the following concerns have been addressed.

1. Overall, this manuscript focuses too much on the method itself but does not put enough weight on the science they have obtained by analyzing the dataset. The current organization is more like an AMT paper instead of an ACP one. The authors are advised to move a certain fraction of the technical part, e.g., the contamination session, into the supplement and expand the scientific findings.

Response 2.1: We agree with both reviewers, and have moved most of the text on contamination factor to the supplement. Quite a lot of revisions and adjustments in the part of “4. Discussion” were made to expand the scientific discussions and findings. Details are referred to *Response 1.11 of Reviewer #1*.

2. The texts in the conclusion part are quite redundant and just a repeat of the issues with applying traditional PMF to CIMS data, especially in the first two paragraphs. This part certainly can be rewritten to be more concise and to deliver key conclusions only.

Response 2.2: In the conclusion part, we combined the first two paragraphs into one short paragraph, and also largely simplified other conclusions, as well as highlighting more the new atmospheric findings, as in *Response 1.12*.

3. (Line 121), “six different pathways” would not be the best word, since OH and NO₃ chemistry would not generally happen at the same time. Although OH radicals can be generated from pinene+ozone chemistry at night, the chances for cross reactions of dimers between peroxy radicals formed from OH chemistry and those from nitrate chemistry are just low, in my mind.

Response 2.3: We agree with both reviewers. To eliminate misunderstandings, we have changed the sentence. Detail are referred to the *Response 1.4*.

4. (Line 220-232), a couple of statements should be clarified. There is a statement of a bin width of 0.02 Th (Line 221). On the other hand, authors state “25 bins per unit mass” for Ranges 1 and 2 and “30 bins per unit mass” for Range 3. What caused the difference? Also, I assume that a larger range of signal region for Range 3 in further analysis was due to a worse shift in mass-to-charge? Lastly, what is the setup for the combined range analysis?

Response 2.4: Thanks for the comments. (1) The bin width in this study is 0.02 Th. To eliminate unnecessary computation of masses without any signal, only masses in the signal region (regions containing meaningful signals) were binned. The peaks get progressively wider with increasing m/z ratio, so at the higher masses of Range 3 we used a wider window for the signal. In this study, the signal region for Range 1 and 2 is between $N - 0.2$ and $N + 0.3$ Th, at integer mass N , and $N - 0.2$ and $N + 0.4$ Th for Range 3 (Figure R4). So the bins per unit mass for Ranges 1 and 2 is $0.5 \text{ Th} / 0.02 \text{ Th} = 25$, and for $0.6 \text{ Th} / 0.02 \text{ Th} = 30$ bins.

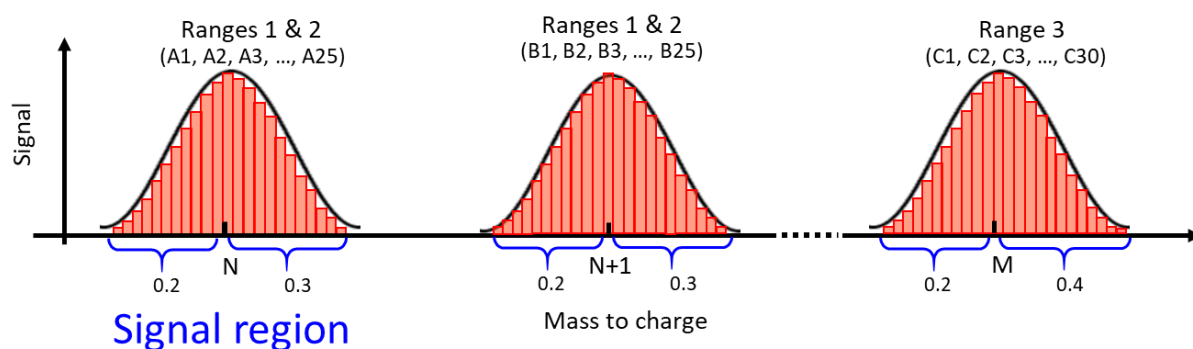


Figure R4 Schematic diagram of data matrix binning process for binPMF analysis. In this study, the bin width is 0.02 Th. For Ranges 1 & 2, the signal region for binning is $[N - 0.2, N + 0.3]$, and for Range 3 is $[N - 0.2, N + 0.4]$.

(2) For the combined range in this analysis, we just combined the mass spectra in the above three ranges, i.e. the three datasets in Ranges 1-3 were combined together to construct combined range. Thus, the highest masses have more bins per integer mass than the mid- and low-mass ranges.

To clarity, we added a statement in Line 240-243:

“To avoid unnecessary computation, only signal regions with meaningful signals in the mass spectra were binned (Zhang et al., 2019). For a nominal mass N , the signal region included in further analyses was between $N-0.2$ Th and $N+0.3$ Th for Range 1 and 2, and between $N-0.2$ Th and $N+0.4$ Th for Range 3. The wider signal regions in Range 3 is due to wider peaks at higher masses. The data were averaged into 1-h time resolution and in total we had 384 time points in the data matrix.”

5. (Sessions 3.2-3.5), since the authors started from two factor analysis to more factors, point out the sequence of factors presented does not necessarily correspond that in the figures in each session.

Response 2.5: We added two sentences in section 3.1 to clarify this.

“..... separately for each Range (sections 3.2 – 3.5). It is worth noting that the factor order in factor evolution does not necessarily correspond to that of the final results. The factor orders displayed in Figures 2-5 have been modified for further comparison between different ranges. More detailed” in Line 288-290.

6. (Figures 2-5), state the time period for the factor contribution.

Response 2.6: The factor contribution is an average from the whole measurement period. For the text, the relative sentence was modified in section 3.2-3.5, respectively, to make this clear.

“..... for further discussion, and Figure 2 shows the result of Range 1, with spectral profile, time series, diurnal cycle and averaged factor contribution during the campaign.....” in Line 313.

“..... Figure 3 shows four-factor result of Range 2, with spectral profile, time series, diurnal cycle and averaged factor contribution during the campaign.” in Line 348-350.

“.....goal in this study. Figure 5 shows the four-factor result of Range Combined, with spectral profile, time series, diurnal cycle and averaged factor contribution during the campaign. The signals in.....” in Line 394-395.

Figure caption in Figure 2-5 were also modified, from “(2) factor contribution” to “(2) averaged factor contribution during the campaign”.

7. (Line 361-362, 455-456), isn't it true that the ultimate source of NO during daytime is still emission?

Response 2.7: Yes, the reviewer is partly correct.

On one hand, the natural source of NO is from lightning stroke, while the anthropogenic sources can be from human activities involving high temperatures, like combustion of fossil fuels.

On the other hand, the monitoring site in this study where we collected the data, Hyytiälä, is located in a boreal forest, with minor anthropogenic emissions (Heikkinen et al., 2019). Nearby sources are two saw mills and a pellet factory 6-7 km away (Äijälä et al., 2019), with no significant emission of NO. The dominant influence of air pollution are still coming from transport from industrialized areas over southern Finland, Russia and the Baltic countries (Riuttanen et al., 2013; Heikkinen et al., 2019). Primary emissions of NO from fossil combustion processes are not long-lived enough to be transported long distances. NO can react with O₃ rapidly to form NO₂, typically on the timescale of minutes. As a result, even though we cannot totally rule out the primary emission of NO during daytime, the photochemical reactions will play the dominant role in NO production. To make the statement more rigorous, revision were made in Line 388:

“During the day, photochemical reactions as well as potential emissions increase the concentration of NO, which serves as peroxy radical (RO₂) terminator and often outcompetes RO₂ cross reactions in which dimers can be formed (Ehn et al., 2014)”.

8. (Line 435), the termination of one peroxy radicals with another does not necessarily have to lead to the formation of dimers.

Response 2.8: As we responded in *Response 1.5*, we agreed with the reviewer that termination of two peroxy radicals doesn't necessarily lead to dimer formation. To clarify the statement, we made revision to the sentence in Line 462-463 to

“This termination step is mutually exclusive with the termination of RO₂ with other RO₂, which can lead to dimer formation.”

9. (Line 497-499), rephrase the sentence.

Response 2.9: The sentence has been removed from the text, to decrease the discussion part of contamination factor.

10. (Session 4.2.1) Although there might not be a daytime factor previously, it is not surprising that dimers are formed in the day. NO channel competes with the self reactions of peroxy radicals but which level of NO will really dominate is still an open question.

Response 2.10: We agree with the reviewer that dimers can be expected to form during daytime, however, the relative studies or results are quite few. For chamber studies, experimental results show that dimer concentration is strongly affected by NO concentration (Ehn et al., 2014). The amount of NO required to hinder dimer formation is also a function of the RO₂ concentrations. In ambient measurement, Mohr et al. (2017) reported a clear diel pattern of dimers with maximum after noon, which is among the first daytime gas-phase dimer observations in the atmosphere, in contrast to the typical daytime minima observed in Hyytiälä (Yan et al., 2016). The NO channel suppresses RO₂ + RO₂ reactions in daytime to a large extent, which leads to lower signals of these daytime dimers to be detected. But definitely, more evidence and studies are needed to reveal and quantify the NO competing ability towards dimer formation in the daytime.

Reference

- Äijälä, M., Daellenbach, K. R., Canonaco, F., Heikkinen, L., Junninen, H., Petäjä, T., Kulmala, M., Prévôt, A. S. H., and Ehn, M.: Constructing a data-driven receptor model for organic and inorganic aerosol – a synthesis analysis of eight mass spectrometric data sets from a boreal forest site, *Atmos. Chem. Phys.*, 19, 3645-3672, 10.5194/acp-19-3645-2019, 2019.
- Bianchi, F., Kurtén, T., Riva, M., Mohr, C., Rissanen, M. P., Roldin, P., Berndt, T., Crounse, J. D., Wennberg, P. O., Mentel, T. F., Wildt, J., Junninen, H., Jokinen, T., Kulmala, M., Worsnop, D. R., Thornton, J. A., Donahue, N., Kjaergaard, H. G., and Ehn, M.: Highly Oxygenated Organic Molecules (HOM) from Gas-Phase Autoxidation Involving Peroxy Radicals: A Key Contributor to Atmospheric Aerosol, *Chemical Reviews*, 119, 3472-3509, 10.1021/acs.chemrev.8b00395, 2019.
- Ehn, M., Thornton, J. A., Kleist, E., Sipila, M., Junninen, H., Pullinen, I., Springer, M., Rubach, F., Tillmann, R., Lee, B., Lopez-Hilfiker, F., Andres, S., Acir, I.-H., Rissanen, M., Jokinen, T., Schobesberger, S., Kangasluoma, J., Kontkanen, J., Nieminen, T., Kurten, T., Nielsen, L. B., Jorgensen, S., Kjaergaard, H. G., Canagaratna, M., Dal Maso, M., Berndt, T., Petaja, T., Wahner, A., Kerminen, V.-M., Kulmala, M., Worsnop, D. R., Wildt, J., and Mentel, T. F.: A large source of low-volatility secondary organic aerosol, *Nature*, 506, 476-479, 10.1038/nature13032, 2014.
- Heikkinen, L., Äijälä, M., Riva, M., Luoma, K., Dällenbach, K., Aalto, J., Aalto, P., Aliaga, D., Aurela, M., Keskinen, H., Makkonen, U., Rantala, P., Kulmala, M., Petäjä, T., Worsnop, D., and Ehn, M.: Long-term sub-micron aerosol chemical composition in the boreal forest: inter- and intra-annual variability, *Atmos. Chem. Phys. Discuss.*, 2019, 1-41, 10.5194/acp-2019-849, 2019.
- Liebmann, J., Karu, E., Sobanski, N., Schuladen, J., Ehn, M., Schallhart, S., Quéléver, L., Hellen, H., Hakola, H., Hoffmann, T., Williams, J., Fischer, H., Lelieveld, J., and Crowley, J. N.: Direct measurement of NO₃ radical reactivity in a boreal forest, *Atmos. Chem. Phys.*, 18, 3799-3815, 10.5194/acp-18-3799-2018, 2018.
- Mohr, C., Lopez-Hilfiker, F. D., Yli-Juuti, T., Heitto, A., Lutz, A., Hallquist, M., D'Ambro, E. L., Rissanen, M. P., Hao, L., Schobesberger, S., Kulmala, M., Mauldin III, R. L., Makkonen, U., Sipilä, M., Petäjä, T., and Thornton, J. A.: Ambient observations of dimers from terpene oxidation in the gas phase: Implications for new particle formation and growth, 44, 2958-2966, 10.1002/2017gl072718, 2017.
- Orlando, J. J., and Tyndall, G. S.: Laboratory studies of organic peroxy radical chemistry: an overview with emphasis on recent issues of atmospheric significance, *J Chemical Society Reviews*, 41, 6294-6317, 2012.

- Peräkylä, O., Riva, M., Heikkinen, L., Quéléver, L., Roldin, P., and Ehn, M.: Experimental investigation into the volatilities of highly oxygenated organic molecules (HOM), *Atmospheric Chemistry and Physics*, 20, 649–669, 10.5194/acp-2019-620, 2020.
- Riuttanen, L., Hulkkonen, M., Dal Maso, M., Junninen, H., and Kulmala, M.: Trajectory analysis of atmospheric transport of fine particles, SO₂, NO_x and O₃ to the SMEAR II station in Finland in 1996–2008, *Atmos. Chem. Phys.*, 13, 2153–2164, 10.5194/acp-13-2153-2013, 2013.
- Riva, M., Ehn, M., Li, D., Tomaz, S., Bourgain, F., Perrier, S., and George, C.: CI-Orbitrap: An Analytical Instrument To Study Atmospheric Reactive Organic Species, *Analytical Chemistry*, 91, 9419–9423, 10.1021/acs.analchem.9b02093, 2019.
- Yan, C., Nie, W., Aijala, M., Rissanen, M. P., Canagaratna, M. R., Massoli, P., Junninen, H., Jokinen, T., Sarnela, N., Hame, S. A. K., Schobesberger, S., Canonaco, F., Yao, L., Prevot, A. S. H., Petaja, T., Kulmala, M., Sipila, M., Worsnop, D. R., and Ehn, M.: Source characterization of highly oxidized multifunctional compounds in a boreal forest environment using positive matrix factorization, *Atmospheric Chemistry and Physics*, 16, 12715–12731, 10.5194/acp-16-12715-2016, 2016.

Insights on Atmospheric Oxidation Processes by Performing Factor Analyses on Sub-ranges of Mass Spectra

YanJun Zhang¹, Otso Peräkylä¹, Chao Yan¹, Liine Heikkinen¹, Mikko Äijälä¹, Kaspar R. Daellenbach¹, Qiaozhi Zha¹, Matthieu Riva^{1,2}, Olga Garmash¹, Heikki Junninen^{1,3}, Pentti Paatero¹, Douglas Worsnop^{1,4}, and Mikael Ehn¹

¹ Institute for Atmospheric and Earth System Research / Physics, Faculty of Science, University of Helsinki, Helsinki, 00014, Finland

² Univ Lyon, Université Claude Bernard Lyon 1, CNRS, IRCELYON, F-69626, Villeurbanne, France

³ Institute of Physics, University of Tartu, Tartu, 50090, Estonia

⁴ Aerodyne Research, Inc., Billerica, MA 01821, USA

Corresponding author: yanjun.zhang@helsinki.fi

Formatted: Font: (Default) Times New Roman

Abstract

With the recent developments in mass spectrometry, combined with the strengths of factor analysis techniques, our understanding of atmospheric oxidation chemistry has improved significantly. The typical approach for using techniques like positive matrix factorization (PMF) is to input all measured data for the factorization in order to separate contributions from different sources and/or processes to the total measured signal. However, while this is a valid approach for assigning the total signal to factors, we have identified several cases where useful information can be lost if solely using this approach. For example, gaseous molecules emitted from the same source can show different temporal behaviors due to differing loss terms, like condensation at different rates due to different molecular masses. This conflicts with one of PMF's basic assumptions of constant factor profiles. In addition, some ranges of a mass spectrum may contain useful information, despite contributing only minimal fraction to the total signal, in which case they are unlikely to have a significant impact on the factorization result. Finally, certain mass ranges may contain molecules formed via pathways not available to molecules in other mass ranges, e.g. dimeric species versus monomeric species. In this study, we attempted to address these challenges by dividing mass spectra into sub-ranges and applying the newly developed binPMF method to these ranges separately. We utilized a dataset from a chemical ionization atmospheric pressure interface time-of-flight (CI-API-TOF) mass spectrometer as an example. We compare the results from these three different ranges, each corresponding to molecules of different volatilities, with binPMF results from the combined range. Separate analysis showed clear benefits in dividing factors for molecules of different volatilities more accurately, in

resolving different chemical processes from different ranges, and in giving a chance for high-molecular-weight molecules with low signal intensities to be used to distinguish dimeric species with different formation pathways. ~~As two major insights from our study, we identified In-addition,~~ daytime dimer formation (diurnal peak around noon) ~~was identified,~~ which may contribute to NPF in Hyytiälä-, ~~as well as Also,~~ dimers from NO₃ oxidation ~~process were separated by the sub-range bin PMF, which would not be identified otherwise.~~ We recommend PMF users to try running their analyses on selected sub-ranges in order to further explore their datasets.

1 Introduction

Huge amounts of volatile organic compounds (VOC) are emitted to the atmosphere every year (Guenther et al., 1995; Lamarque et al., 2010), which play a significant role in atmospheric chemistry and affect the oxidative ability of the atmosphere. The oxidation products of VOC can contribute to the formation and growth of secondary organic aerosols (Kulmala et al., 2013; Ehn et al., 2014; Kirkby et al., 2016; Troestl et al., 2016), affecting air quality, human health, and climate radiative forcing (Pope III et al., 2009; Stocker et al., 2013; Zhang et al., 2016; Shiraiwa et al., 2017). Thanks to the advancement in mass spectrometric applications, like the aerosol mass spectrometer (AMS) (Canagaratna et al., 2007) and chemical ionization mass spectrometry (CIMS) (Bertram et al., 2011; Jokinen et al., 2012; Lee et al., 2014) our capability to detect these oxidized products, as well as our understanding of the complicated atmospheric oxidation pathways in which they take part, have been greatly enhanced.

Monoterpenes (C₁₀H₁₆), one common group of VOC emitted in forested areas, have been shown to be a large source of atmospheric secondary organic aerosol (SOA). The oxidation of monoterpenes produces a wealth of different oxidation products (Oxygenated VOC, OVOC), including highly oxygenated organic molecules (HOM) with molar yields in the range of a few percent, depending on the specific monoterpene and oxidant (Ehn et al., 2014; Bianchi et al., 2019). Bianchi et al. (2019) summarized that HOM can be either Extremely Low Volatility Organic Compounds (ELVOC), Low Volatility Organic Compounds (LVOC), or Semi-volatile Organic Compounds (SVOC) (classifications by Donahue et al. 2012), depending on their exact structures. For less oxygenated products, the majority are likely to fall into the SVOC or the Intermediate VOC (IVOC) range. The volatility of the OVOC will determine their dynamics, including their ability to contribute to the formation of SOA and new particles (Bianchi et al., 2019; Buchholz et al., 2019).

The recent developments of CIMS techniques has allowed researchers to observe unprecedented numbers of OVOC, in real-time (Riva et al., 2019). This ability to measure thousands of compounds is a great benefit, but also a large challenge for the data analyst. For this reason, factor analytical

Field Code Changed

Field Code Changed

Field Code Changed

Field Code Changed

Field Code Changed

Field Code Changed

Field Code Changed

Field Code Changed

Field Code Changed

68 techniques have often been applied to reduce the complexity of the data by finding co-varying signals
69 that can be grouped into common factors (Huang et al., 1999). For aerosol and gas-phase mass
70 spectrometry, positive matrix factorization, PMF (Paatero and Tapper, 1994; Zhang et al., 2011) has
71 been the most utilized tool. The factors have then been attributed to sources (e.g. biomass burning
72 organic aerosol) or processes (e.g. monoterpene ozonolysis) depending on the application and ability
73 to identify spectral signatures (Yan et al., 2016; Zhang et al., 2017). In the vast majority of these PMF
74 applications to mass spectra, the mass range of ions has been maximized in order to provide as much
75 input as possible for the algorithm. This approach was certainly motivated in early application of
76 PMF on e.g. offline filters, with chemical information of metals, water-soluble ions, and organic and
77 elemental carbon (OC and EC), where the number of variables is counted in tens, and the number of
78 samples in tens or hundreds (Zhang et al., 2017). However, with gas-phase CIMS, we often have up
79 to a thousand variables, with hundreds or even thousands of samples, meaning that the amount of data
80 itself is unlikely to be a limitation for PMF calculation. In this work, we aimed to explore potential
81 benefits of dividing the spectra into sub-ranges before applying factorization analysis.

82 An inherent requirement of factorization approaches is that the factor profiles, in this case the relative
83 abundances of ions in the mass spectra, of each factor stay nearly constant. Due to the complexity
84 and number of atmospheric processes affecting the formation, transformation, and loss of VOC,
85 OVOC and aerosol, this often does not hold, and is one of the main limitations of factorization
86 approaches. Given the different volatilities of OVOC, it may even be expected that molecules from
87 the same source may have very different loss time scales, which may affect the factor analysis. For
88 compounds of low volatility, such as many HOM, the main atmospheric loss process is typically
89 condensation onto aerosol particles, with chemical sink being negligible (Bianchi et al., 2019). If, on
90 the other hand, a compound does not irreversibly condense, oxidation reactions can also affect its
91 lifetime. Volatility issue has been studied and reported for AMS data, with different volatilities of
92 various OA types (Huffman et al., 2009; Crippa et al., 2014; Paciga et al., 2016; Äijälä et al., 2017).
93 Semi-volatile oxygenated organic aerosol (SV-OOA) and Low-volatility oxygenated organic aerosol
94 (LV-OOA) can both be mainly produced from biogenic sources, but get separated based on different
95 volatilities by PMF (El Haddad et al., 2013). Sekimoto et al. (2018) found that the two profiles
96 resolved with VOC emitted from biomass burning had different estimated volatilities. As the
97 volatility of a molecule is linked to its molecular mass (Peräkylä et al., 2020), it may be beneficial to
98 apply PMF separately to mass ranges where one can expect the loss processes to be similar, thereby
99 resulting in more constant factor profiles. In this way, distinct sources are hopefully separated by
100 PMF, with minimized influence of differing volatilities from one source.

Field Code Changed

Field Code Changed

Field Code Changed

Field Code Changed

Formatted: Font color: Auto

Field Code Changed

Field Code Changed

Field Code Changed

Field Code Changed

The number of PMF or other factorization studies utilizing CIMS data remains very limited. “Traditional” PMF analyses have so far, to our knowledge, only been applied to nitrate-based chemical ionization atmospheric pressure interface time-of-flight (CI-API-TOF) data (Yan et al., 2016; Massoli et al., 2018). One study has also utilized non-negative matrix factorization (NNMF) to look at diurnal trends of Iodide ToF-CIMS data (Lee et al., 2018). The lack of more studies utilizing PMF, or other factorization techniques, on CIMS data is likely partly due to the complexity of the data, with multiple overlapping ions hampering HR peak fitting (Zhang et al., 2019). In addition, variable factor profiles may hamper PMF’s ability to correctly separate the factors. The two CI-API-TOF studies utilized the nearly the entire measured spectrum (from around 200 Th to around 600 Th), either in unit mass resolution (UMR) or high resolution (HR) peak fitting data (Yan et al., 2016; Massoli et al., 2018). Massoli et al. (2018) estimated the volatility of the molecules they detected, finding that all the six extracted factors had notable contributions from IVOC, SVOC and (E)LVOC. These compound groups will have clearly different loss mechanisms, and thereby loss rates, suggesting that variation in factor profiles is inevitable, even if the source was identical for all molecules in the factor. We hypothesize that this effect further hampers the correct factorization, and further that this effect can be reduced by dividing the spectra into separate ranges, with each sub-range containing molecules with roughly similar loss mechanisms and rates.

As an additional motivation to separate different ranges from the mass spectrum, it is not only the loss mechanisms, but also the formation pathways that may differ. For example, atmospheric oxidation chemistry of organics is, to a large extent, the chemistry of peroxy radicals (RO_2) (Orlando and Tyndall, 2012). These RO_2 are initiated by VOC reacting with oxidants like ozone, or the hydroxyl (OH) or nitrate (NO_3) radicals, while their termination occurs mainly by bimolecular reactions with NO, HO_2 and/or other RO_2 . Some product molecules can be formed from many of the three termination pathways, while for example ROOR “dimers” can only be formed from $\text{RO}_2 + \text{RO}_2$ reactions (Berndt et al., 2018a; Berndt et al., 2018b). This also means that there can be several different pathways to form dimers from the same precursors VOC, by combining RO_2 formed from the same or different oxidants. As an example of the latter, an ROOR dimer can contain one moiety produced from ozone oxidation and another moiety from NO_3 oxidation (Yan et al., 2016). Thus, their concentration is dependent on both the precursor VOC concentration, and the concentrations of both oxidants. Such a molecule will not have a direct equivalent in any of the monomer products; even though monomers can form from $\text{RO}_2 + \text{R}'\text{O}_2$ reactions, the products from RO_2 are not dependent on the source of the $\text{R}'\text{O}_2$. This may complicate the identification of certain dimer factors by PMF if the entire spectrum is analyzed at once, and therefore separation of the monomer and dimer products before the PMF analysis could be advantageous.” Such a molecule will not have a direct

Field Code Changed

Field Code Changed

Field Code Changed

Field Code Changed

Field Code Changed

Field Code Changed

Field Code Changed

Formatted: Font color: Auto

Formatted: No underline, Font color: Auto

Formatted: Font color: Auto

Formatted: Font color: Auto

equivalent in any of the monomer products, dependent on only one oxidant, which again may complicate the separation of such factors by PMF, if the entire spectrum is analyzed once. However, if separating the monomer and dimer products before PMF analysis, separation of different formation pathways can potentially become simpler.

Recently, we proposed a new PMF approach, binPMF, to simplify the analysis of mass spectral data (Zhang et al., 2019). This method divides the mass spectrum into narrow bins, typically some tens of bins per integer mass, depending on the mass resolving power of the instrument, before performing PMF analyses. In this way, binPMF does not require any time-consuming, and potentially subjective high resolution peak fitting, and can thus be utilized for data exploration at a very early stage of data analysis. Data preparation is nearly as simple as in the case of UMR analysis, yet it utilizes much more spectral information as it does not sum up signal over all ions at each integer mass. In addition to saving time and effort in data analysis, the results are less sensitive to mass calibration fluctuations. Finally, the binning also greatly increases the number of input variables, which has the advantage that factor analysis with smaller mass ranges becomes more feasible, as more meaningful variation is supplied to the algorithm.

We designed this study to explore the benefits of separate analysis of different mass ranges from mass spectra. We used a previously published ambient dataset measured by a CI-API-TOF, and conducted binPMF analysis with three different mass ranges, roughly corresponding to different volatility ranges. We compared the results from the sub-range analyses with each other and with results from binPMF run on the combined ranges. We found that dimers generated during daytime and dimers initiated by NO₃ oxidation can be separated from our dataset by utilizing the sub-ranges, but not with the full range. We believe~~We found that more meaningful factors are separated from our dataset by utilizing the sub-ranges, and believe~~ that this study will provide new perspectives for future studies analyzing gas-phase CIMS data.

2 Methodology

The focus of this work is on retrieving new information from mass spectra by applying new analytical approaches. Therefore, we chose a dataset that has been presented earlier, though without PMF analysis, by Zha et al. (2018), and was also used in the first study describing the binPMF method (Zhang et al., 2019). The measurements are described in more details below in section 2.1, while the data analysis techniques used in this work are presented in section 2.2.

2.1 Measurements

2.1.1 Ambient site

Field Code Changed

Formatted: Font color: Auto

Formatted: No underline, Font color: Auto

Formatted: No underline, Font color: Auto

Field Code Changed

Field Code Changed

Formatted: Font: Bold

169 The ambient measurements were conducted at the Station for Measuring Ecosystem–Atmosphere
170 Relations (SMEAR) II in Finland (Hari and Kulmala, 2005) as part of the Influence of Biosphere-
171 Atmosphere Interactions on the Reactive Nitrogen budget (IBAIRN) campaign (Zha et al, 2018).
172 Located in the boreal environment in Hyytiälä, SMEAR II is surrounded with coniferous forest and
173 has limited anthropogenic emission sources nearby. Diverse measurements of meteorology, aerosol
174 and gas phase properties are continuously conducted at the station. Details about the meteorological
175 conditions and temporal variations of trace gases during IBAIRN campaign are presented by Zha et
176 al. (2018) and Liebmann et al. (2018).

Field Code Changed

Field Code Changed

177
178 **2.1.2 Instrument and data**

Formatted: Font: Bold

179 Data were collected with a nitrate (NO_3^-)-based chemical ionization atmospheric pressure interface
180 time-of-flight mass spectrometer (CI-API-TOF, Jokinen et al., 2012) with about 4000 Th Th^{-1} mass
181 resolving power, at ground level in September, 2016. In our study, the mass spectra were averaged to
182 1 h time resolution from September 6th to 22nd for further analysis. We use the thomson (Th) as the
183 unit for mass/charge, with 1 Th = 1 Da/e, where e is the elementary charge. As all the data discussed
184 in this work are based on negative ion mass spectrometry, we will use the absolute value of the
185 mass/charge, although the charge of each ion will be negative. The masses discussed in this work
186 includes the contribution from the nitrate ion, 62, unless specifically mentioned. Furthermore, as the
187 technique is based on soft ionization with NO_3^- ions, any multiple charging effects are unlikely, and
188 therefore the reported mass/charge values in thomson can be considered equivalent to the mass of the
189 ion in Da.

Formatted: Font: (Default) Times New Roman

190 The forest site of Hyytiälä is dominated by monoterpene emissions (Hakola et al., 2006). The main
191 feature of previous CI-API-TOF measurements in Hyytiälä (Ehn et al., 2014; Yan et al., 2016) has
192 been a bimodal distributions of HOM, termed monomers and dimers, as they are formed of either one
193 or two RO_2 radicals, respectively. For the analysis in this study, we chose three mass/charge (m/z)
194 ranges of 50 Th each (Figure 1), corresponding to regions between which we expect differences in
195 formation or loss mechanisms. In addition to regions with HOM monomers and HOM dimers, one
196 range was chosen at lower masses, in a region presumably mainly consisting of molecules that are
197 less likely to condense onto aerosol particles (Peräkylä et al., 2020).

Field Code Changed

Field Code Changed

Field Code Changed

198
199 **2.2 Positive matrix factorization (PMF)**

Formatted: Font: Bold

200 After the model of PMF was developed (Paatero and Tapper, 1994), numerous applications have been
201 conducted with different types of environmental data (Song et al., 2007; Ulbrich et al., 2009; Yan et
202 al., 2016; Zhang et al., 2017). By reducing dimensionality of the measured dataset, PMF model greatly

Field Code Changed

Field Code Changed

simplifies the data analysis process with no requirement for prior knowledge of sources or pathways as essential input. The main factors can be further interpreted with their unique/dominant markers (elements or masses).

The basic assumption for PMF modelling is mass balance, which assumes that ambient concentration of a chemical component is the sum of contributions from several sources or processes, as shown in equation (1).

$$\mathbf{X} = \mathbf{TS} \times \mathbf{MS} + \mathbf{R} \quad (1)$$

In equation (1), \mathbf{X} stands for the time series of measured concentration of different variables (m/z in our case), \mathbf{TS} represents the temporal variation of factor contributions, \mathbf{MS} stands for factor profiles (mass spectral profiles), and \mathbf{R} is the residual as the difference of the modelled and the observed data. The matrices \mathbf{TS} and \mathbf{MS} are iteratively calculated by a least-squares algorithm utilizing uncertainty estimates, to pursue minimized Q value as shown in equation (2), where S_{ij} is the estimated uncertainty, an essential input in PMF model.

$$Q = \sum \sum \left(\frac{R_{ij}}{S_{ij}} \right)^2 \quad (2)$$

PMF model was conducted by multi-linear engine (ME-2) (Paatero, 1999) interfaced with Source Finder (SoFi, v6.3) (Canonaco et al., 2013). Signal-to-noise ratio (SNR) was calculated as $\text{SNR}_{ij} = \text{abs}(X_{ij}) / \text{abs}(S_{ij})$. When the Signal-to-noise ratio (SNR) is below 1, the signal of X_{ij} will be down-weighted by replacing the corresponding uncertainty S_{ij} by S_{ij}/SNR_{ij} (Visser et al., 2015). Future studies should pay attention to the potential risk when utilizing this method since down-weighting low signals element-wise will create a positive bias to the data. Robust mode was operated in the PMF modelling, where outliers ($\left| \frac{R_{ij}}{S_{ij}} \right| > 4$) were significantly down-weighted (Paatero, 1997).

2.3 binPMF

As a newly developed application of PMF for mass spectral data, binPMF has no requirement for chemical composition information, while still taking advantage of the HR mass spectra, saving effort and time (Zhang et al., 2019). To explore the benefits of analyzing separated mass ranges, we applied binPMF to the three separated ranges. The three ranges were also later combined for binPMF analysis as comparison with the previous results. The PMF model requires both data matrix and error matrix as input, and details of the preparation of data and error matrices are described below.

2.3.1 Data matrix

Field Code Changed

Field Code Changed

Field Code Changed

Formatted: Font: Bold

Field Code Changed

Formatted: Font: Bold

234 Different from normal UMR or HR peak fitting, in binPMF, the mass spectra are divided into small
 235 bins after baseline subtraction and mass axis calibration. Linear interpolation was first conducted to
 236 the mass spectra with a mass interval of 0.001 Th. Then the interpolated data was averaged into bins
 237 of 0.02 Th width. We selected three ranges for further analysis based on earlier studies (Ehn et al.,
 238 2014; Yan et al., 2016; Bianchi et al., 2019; Peräkylä et al., 2020).

- 239 - Range 1, m/z 250 – 300 Th, 51 unit masses \times 25 bins per unit mass = 1275 bins/variables,
 240 consisting mainly of molecules with five to nine carbon atoms and four to nine oxygen atoms
 241 in our dataset.
- 242 - Range 2, m/z 300 – 350 Th, $51 \times 25 = 1275$ bins, mainly corresponding to HOM monomer
 243 products, featured with nine to ten C- and seven to ten O-atoms.
- 244 - Range 3, m/z 510 – 560 Th, $51 \times 30 = 1530$ bins, mainly corresponding to HOM dimer products,
 245 with carbon numbers of sixteen to twenty and eleven to fifteen O-atoms.

246 To avoid unnecessary computation, only signal regions with meaningful signals in the mass spectra
 247 were binned (Zhang et al., 2019). For a nominal mass N , the signal region included in further analyses
 248 was between $N-0.2$ Th and $N+0.3$ Th for Range 1 and 2, and between $N-0.2$ Th and $N+0.4$ Th for
 249 Range 3. The wider signal regions in Range 3 is due to wider peaks at higher masses. The data were
 250 averaged into 1-h time resolution and in total we had 384 time points in the data matrix.

252 2.3.2 Error matrix

253 The error matrix represents the estimated uncertainty for each element of the data matrix and is crucial
 254 for iterative calculation of the Q minimum. Equation (3) is used for error estimation (Polissar et al.,
 255 1998),

$$256 S_{ij} = \sigma_{ij} + \sigma_{\text{noise}} \quad (3)$$

257 where S_{ij} represents the uncertainty of m/z j at time i , σ_{ij} stands for counting statistics uncertainty
 258 and is estimated as follows,

$$259 \sigma_{ij} = a \times \frac{\sqrt{I_{ij}}}{\sqrt{t_s}} \quad (4)$$

260 where I is the signal intensity term, in unit of counts per second (cps), t_s stands for length of averaging
 261 in seconds, while a is an empirical coefficient to compensate for unaccounted uncertainties (Allan et
 262 al., 2003; Yan et al., 2016) and is 1.28 in our study as previously estimated from laboratory
 263 experiments (Yan et al., 2016). The σ_{noise} term was estimated as the median of the standard
 264 deviations from signals in the bins in the region between nominal masses, where no physically
 265 meaningful signals are expected.

Field Code Changed

Formatted: Font color: Text 1

Formatted: No underline, Font color: Text 1

Formatted: Font color: Text 1

Formatted: No underline

Formatted: Font color: Text 1

Formatted: Font: Bold

Field Code Changed

Field Code Changed

3 Results

3.1 General overview of the dataset/spectrum

During the campaign, in autumn, 2016, the weather was overall sunny and humid with average temperature of 10.8 °C and relative humidity (RH) of 87% (Zha et al., 2019). The average concentration of NO_x and O₃ was 0.4 ppbv and 21 ppbv, respectively. The average total HOM concentration was ~ 10⁸ molecules cm⁻³.

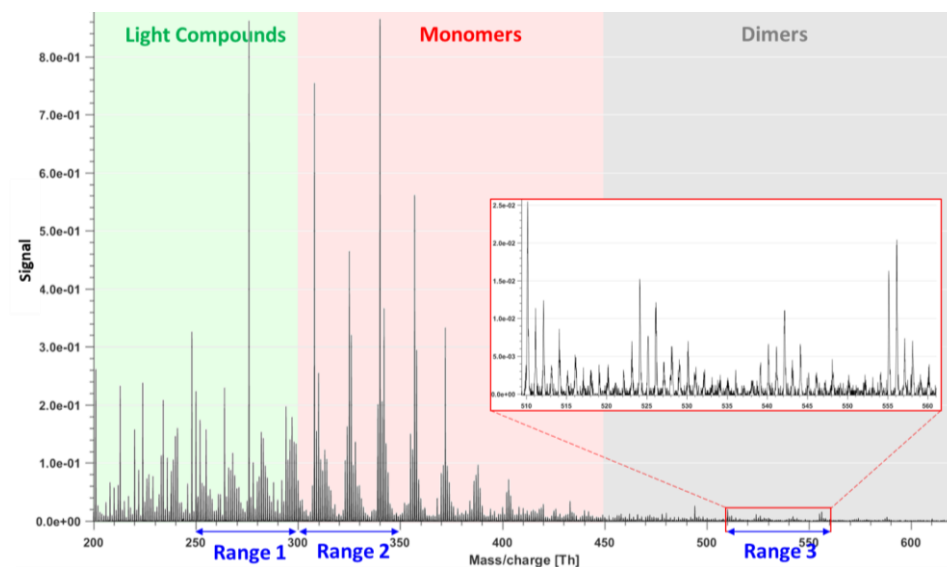


Figure 1. Example of mass spectrum with 1-h time resolution measured from a boreal forest environment during the IBAIRN campaign (at 18:00, Finnish local time, UTC+2). The mass spectrum was divided into three parts and three sub-ranges were chosen from different parts for further analysis in our study. The nitrate ion (62 Th) is included in the mass.

Figure 1 shows the 1 h averaged mass spectrum taken at 18:00 on September 12, as an example of the analyzed dataset. In addition to exploring the benefits of this type of sub-range analysis in relation to different formation or loss pathways, separating into sub-ranges may also aid factor identification for low-signal regions. As shown in Figure 1, there is a difference of 1-2 orders of magnitude in the signal intensity between Range 3 and Ranges 1-2. If all Ranges are run together, we would expect that the higher signals from Ranges 1 and 2 will drive the factorization. While if run separately, separating formation pathways of dimers in Range 3 will likely be easier. As dimers have been shown to be crucial for the formation of new aerosol particles from monoterpene oxidation (Kirkby et al.,

Formatted: Font: Bold

Formatted: Font: 11 pt

Field Code Changed

2016;Troestl et al., 2016;Lehtipalo et al., 2018), this information may even be the most critical in some cases, despite the low contribution of these peaks to the total measured signal. binPMF was separately applied to Range 1, 2, 3, and a ‘Range combined’ which comprised all the three sub-ranges. All the PMF runs for the four ranges were conducted from two to ten factors and repeated three times for each factor number, to assure the consistency of the results. Factorization results and evolution with increasing factor number are briefly described in the following sections, separately for each Range (sections 3.2 – 3.5). It is worth noting that the factor order in factor evolution does not necessarily correspond to that of the final results. The factor orders displayed in Figures 2-5 have been modified for further comparison between different ranges. More detailed discussion and comparison between the results are presented in Section 4.

3.2 binPMF on Range 1 (250 – 300 Th)

As has become routine (Zhang et al., 2011;Craven et al., 2012), we first examined the mathematical parameters of our solutions. From two to ten factors, Q/Q_{exp} decreased from 2.8 to 0.7 (Fig S1 in supplementary information), and after three factors, the decreasing trend was gradually slowing down and approaching one, which is the ideal value for Q/Q_{exp} as a diagnostic parameter. The unexplained variation showed a decline from 18% to 8% from two to ten factors.

In the two-factor results, two daytime factors were separated, with peak time both at 14:00 - 15:00. One factor was characterized by large signals at 250 Th, 255 Th, 264 Th, 281 Th, 283 Th, 295 Th, 297 Th. The other factor was characterized by large signals at 294 Th, 250 Th, 252 Th, 264 Th, 266 Th, 268 Th, and 297 Th. In Hyytiälä, as reported in previous studies, odd masses observed by the nitrate CI-API-TOF are generally linked to monoterpene-derived organonitrates during the day (Ehn et al., 2014;Yan et al., 2016). When the factor number increased to three, the two earlier daytime factors remained similar with the previous result, while a new factor appeared with a distinct sawtooth shape in the diurnal cycle. The main marker in the spectral profile was 276 Th, with a clear negative mass defect. When one more factor was added, the previous three factors remained similar as in the three-factor solution, and a new morning factor was resolved, with 264 Th and 297 Th dominant in the mass spectral profile, and a diurnal peak at 11:00.

As the factor number was increased, more daytime factors were separated, with similar spectral profiles to existing daytime factors and various peak times. No nighttime factors were found in the analysis even when the factor number reached ten. We chose the four-factor result for further discussion, and Figure 2 shows the result of Range 1, with spectral profile, time series, diurnal cycle and averaged factor contribution during the campaign~~factor contribution~~. As shown in Figure 2d, Factors 1-3 are all daytime factors, while Factor 4 has no clear diurnal cycle, but a distinct sawtooth

Formatted: English (United States)

Formatted: Font: Bold

Field Code Changed

Field Code Changed

shape. Factor 4 comes from a contamination of perfluorinated acids while Factor 4 has a sawtooth shape, which is caused by contamination, mainly by perfluorinated acids, of from the inlet's automated zeroing every three hours during the measurements (Zhang et al., 2019). The zeroing periods have been removed from the dataset before binPMF analysis, but the contamination factor was still resolved. This factor is discussed in more detail in sections 4.1.1 and 4.1.4.

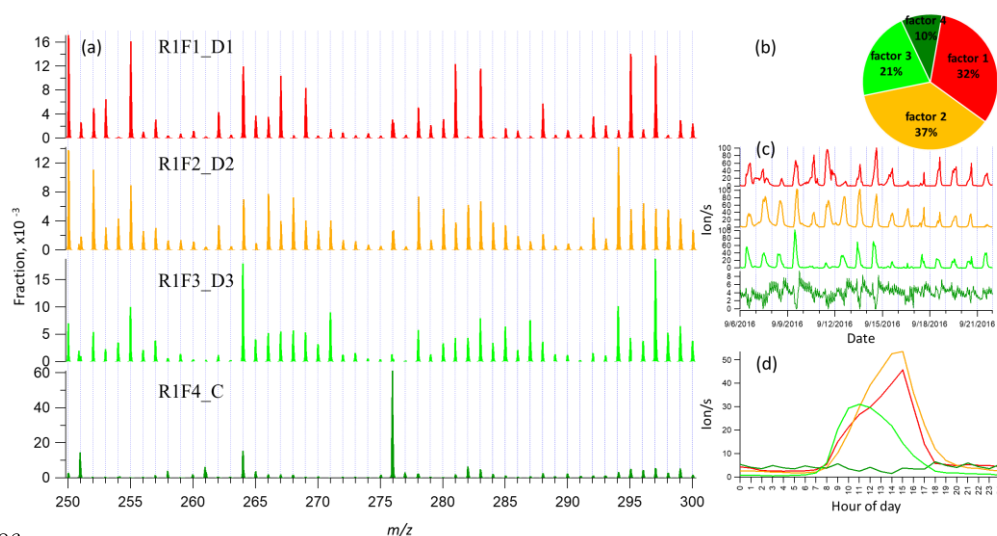


Figure 2 Four-factor result for Range 1, for (a) factor spectral profiles, (b) averaged factor contribution during the campaign, (c) time series and (d) diurnal trend. Details on the factors' naming schemes are shown in Table 1.

3.3 binPMF on Range 2 (300-350 Th)

This range covers the monoterpene HOM monomer range, and binPMF results have already been discussed by Zhang et al. (2019) as a first example of the application of binPMF on ambient data. Our input data here is slightly different. In the previous study, the 10 min automatic zeroing every three hours was not removed before averaging to 1 hour time resolution while here, we have removed this data. Overall, the results are similar as in our earlier study, and therefore the result are just briefly summarized below for further comparison and discussion in Section 4. Similar to Range 1, both the Q/Q_{exp} (2.2 to 0.6) and unexplained variation (16% to 8%) declined with the increased factor number from two to ten.

When the factor number was two, one daytime and one nighttime factor were separated, with diurnal peak times at 14:00 and 17:00, respectively. The nighttime factor was characterized by masses at 340

Formatted: Font: 11 pt

Formatted: Font: 11 pt

Formatted: Font: 10 pt

Formatted: Font: Bold

Th, 308 Th and 325 Th (monoterpene ozonolysis HOM monomers (Ehn et al., 2014)) and remained stable throughout the factor evolution from two to ten factors. With the addition of more factors, no more nighttime factors got separated while the daytime factor was further separated and more daytime factors appeared, peaking at various times in the morning (10:00 am), at noon or in the early afternoon (around 14:00 pm and 15:00 pm). High contribution of 339 Th can be found in all the daytime factor profiles. As the factor number reached six, a contamination factor appeared, characterized by large signals at 339 Th and 324 Th, showing negative mass defects (Figure S2 in the Supplement). The factor profile is nearly identical to the contamination factor determined in Zhang et al. (2019), where the zeroing periods were not removed, causing larger signals for the contaminants. In our dataset, where the zeroing periods were removed, no sawtooth pattern was discernible in the diurnal trend, yet it could still be separated even though it only contributed 3% to Range 2. More about the contamination factors from different ranges will be discussed in Section 4.1.4. Since the aim of this study is mainly to explore the benefits of analyzing different ranges of the mass spectrum, we chose to show the four-factor result below, to simplify the later discussion and comparison. Figure 3 shows four-factor result of Range 2, with spectral profile, time series, diurnal cycle and averaged factor contribution during the campaign.

Field Code Changed

Formatted: No underline, Font color: Auto

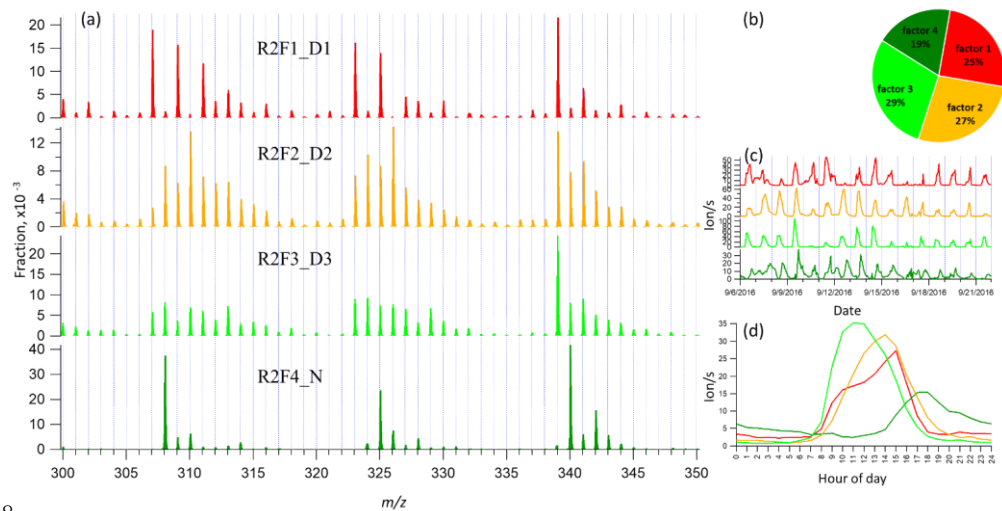


Figure 3 Four-factor result for Range 2, for (a) factor spectral profiles, (b) averaged factor contribution during the campaign, (c) time series and (d) diurnal trend. Details on the factors' naming schemes are shown in Table 1.

Formatted: Font: 11 pt

Formatted: Font: 11 pt

3.4 binPMF on Range 3 (510-560 Th)

Formatted: Font: Bold

Range 3 represents mainly the monoterpene HOM dimers (Ehn et al., 2014). Similar to Range 1 and 2, both the Q/Q_{exp} (1.5 to 0.6) and unexplained variation (18% to 15%) showed decreasing trend with the increased factor number (2-10). As can be seen from Figure 1, data in Range 3 had much lower signals, compared to that of the Range 1 and 2, explaining the higher unexplained variation for Range 3.

In the two-factor result for Range 3, one daytime and one nighttime factor appeared, with diurnal peak times at noon and 18:00, respectively. The nighttime factor was characterized by ions at 510 Th, 524 Th, 526 Th, 542 Th, and 555 Th, 556 Th, while the daytime factor showed no dominant marker masses, yet with relatively high signals at 516 Th, 518 Th and 520 Th. As the number of factors increased to three, one factor with almost flat diurnal trend was separated, with dominant masses of 510 Th, 529 Th, 558 Th. Most peaks in this factor had negative mass defects, and this factor was again linked to a contamination factor. The four-factor result resolved another nighttime factor with a dominant peak at 555 Th, and effectively zero contribution during daytime. As the factor number was further increased, the new factors seemed like splits from previous factors with similar spectral profiles. We therefore chose four-factor result also for Range 3 (results shown in Fig. 4) for further discussion.

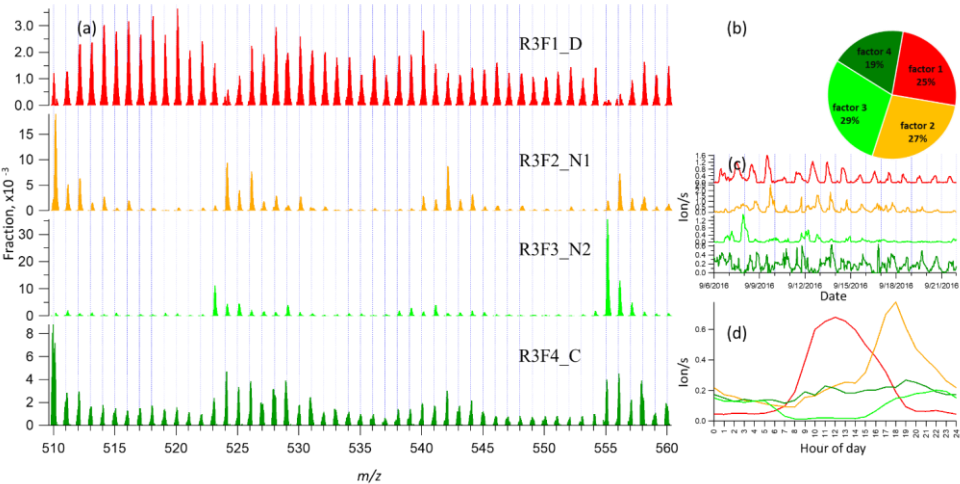


Figure 4 Four-factor result for Range 3, for (a) factor spectral profiles, (b) averaged factor contribution during the campaign, (c) time series and (d) diurnal trend. Details on the factors' naming schemes are shown in Table 1.

3.5 binPMF on Range Combined (250-350 Th & 510-560 Th)

Formatted: Font: 11 pt

Formatted: Left

Formatted: Font: 11 pt

Formatted: Font: Bold

386 As comparison to the previous three ranges, we conducted the binPMF analysis on Range Combined,
387 which is the combination of the three ranges. The results of this range are fairly similar to those of
388 Ranges 1 and 2, as could be expected since the signal intensities in these ranges were much higher
389 than in Range 3. As the number of factors increased (2-10), both the Q/Q_{exp} (1.3 to 0.6) and
390 unexplained variation (16% to 8%) showed a decreasing trend.

391 In the two-factor result, one daytime factor and one nighttime factor were separated. In the nighttime
392 factor, most masses were found at even masses, and the fraction of masses in Range 3 was much
393 higher than that in daytime factor. In contrast, in the daytime factor, most masses were observed at
394 odd masses and the fraction of signal in Range 3 was much lower. During the day, photochemical
395 reactions increase the concentration of NO, which serves as peroxy radical (RO₂) terminator and often
396 outcompetes RO₂ cross reactions in which dimers can be formed (Ehn et al., 2014). Thus, the
397 production of dimers is suppressed during the day, yielding instead a larger fraction of organic nitrates,
398 as has been shown also previously (Yan et al., 2016).

399 With the increase of the number of factors, more daytime factors were resolved with different peak
400 times. When the factor number reached seven, a clear sawtooth-shape diurnal cycle occurred, i.e. the
401 contamination factor, caused by the zeroing. As more factors were added, no further nighttime factors
402 were separated, and only more daytime factors appeared. To simplify the discussion and inter-range
403 comparison, we also here chose the four-factor result for further analysis, as it already provided
404 enough information for our main goal in this study. Figure 5 shows the four-factor result of Range
405 Combined, with spectral profile, time series, diurnal cycle ~~and~~ and averaged factor contribution
406 during the campaign. factor contribution. The signals in range of 510-560 Th were enlarged 100-fold
407 to be visible.

Field Code Changed

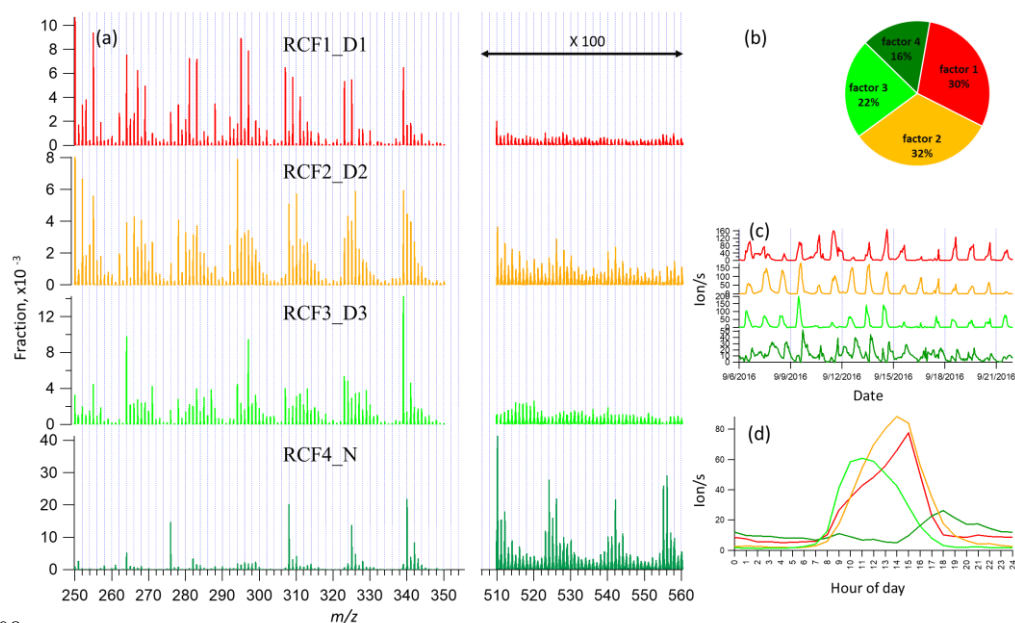


Figure 5 Four-factor result for Range Combined, for (a) factor spectral profiles, (b) averaged factor contribution during the campaign, (c) time series and (d) diurnal trend. Details on the factors' naming schemes are shown in Table 1.

4 Discussion

In Section 3, results by binPMF analysis were shown for Ranges 1, 2, 3 and Combined. In this section, we discuss and compare the results from the different ranges. To simplify the inter-range comparison, we chose four-factor results for all the four ranges, with the abbreviations shown in Table 1. From Range 1, three daytime factors and a contaminations factor were separated. In Range 2, three daytime factors and one nighttime factor (abbreviated as R2F4_N) were resolved. The R2F4_N factor was characterized by signals at 308 Th ($C_{10}H_{14}O_7NO_3^-$), 325 Th ($C_{10}H_{15}O_8NO_3^-$), and 340 Th ($C_{10}H_{14}O_9NO_3^-$), and can be confirmed as monoterpene ozonolysis products (Ehn et al., 2014; Yan et al., 2016). With the increase of factor number to six, the contamination factor got separated also in this mass range. In Range 3, one daytime factor, two nighttime factors and a contamination factor were separated. The first nighttime factor (R3F2_N1) had large peaks at 510 Th ($C_{20}H_{32}O_{11}NO_3^-$) and 556 Th ($C_{20}H_{30}O_{14}NO_3^-$), dimer products that have been identified during chamber studies of monoterpene ozonolysis (Ehn et al., 2014). The molecule observed at 510 Th has 32 H-atoms, suggesting that one of the RO₂ involved would have been initiated by OH, which is formed during

Formatted: Font: 11 pt

Formatted: Font: 11 pt

Field Code Changed

Field Code Changed

the ozonolysis of alkenes such as monoterpenes at nighttime (Atkinson et al., 1992;Paulson and Orlando, 1996). The other nighttime factor (R3F3_N2) was dominated by ions at 523 Th ($C_{20}H_{31}O_8NO_3^+NO_3^-$) and 555 Th ($C_{20}H_{31}O_{10}NO_3^+NO_3^-$), representing nighttime monoterpene oxidation involving NO_3 . As these dimers contain only one N-atom, and 31 H-atoms, we can assume that they are formed from reactions between an RO_2 formed from NO_3 oxidation and another RO_2 formed by ozone oxidation. These results match well with the profiles in a previous study by Yan et al. (2016). The results of Range Combined are very similar to Range 2, with one nighttime factor and three daytime factors. The contamination factor was separated with increase of factor number to seven.

Table 1. Summary of PMF results for the different mass ranges

Range	Factor number	Factor name ^a	Dominant peaks	Peak time
1 (250 - 300 Th)	1	R1F1_D1	250, 255, 295, 297	15:00
	2	R1F2_D2	250, 252, 294	15:00
	3	R1F3_D3	264, 297	11:00
	4	R1F4_C	276	^b
2 (300 - 350 Th)	1	R2F1_D1	307, 309, 323, 325, 339,	15:00
	2	R2F2_D2	310, 326, 339,	14:00
	3	R2F3_D3	339	11:00
	4	R2F4_N	308, 325, 340	18:00
3 (510 – 560 Th)	1	R3F1_D	516, 518, 520, 528, 540	12:00
	2	R3F2_N1	510, 524, 542, 556	18:00
	3	R3F3_N2	523, 555	22:00
	4	R3F4_C	510, 558	^b
Combined (1, 2, 3)	1	RCF1_D1	250, 255, 295, 339	15:00
	2	RCF2_D2	250, 252, 294, 339	14:00
	3	RCF3_D3	264, 297, 339	11:00
	4	RCF4_N	308, 340, 510, 524, 555, 556	18:00

Field Code Changed

Formatted: Font: 11 pt

Formatted: Font: Bold

^a Factor name is defined with range name, factor number and name. For example, RxFy represents Factor y in Range x. RC stands for Range Combined. For the factor name, D is short for daytime, N for Nighttime, C for contamination.

^b The contamination factor in Range 1 shows sawtooth pattern; while in Range 3 shows no diurnal pattern.

4.1 Comparison of different ranges

4.1.1 Time series correlation

In Figure 6, the upper panels show the time series correlations among the first three ranges. As expected based on the results above, generally the daytime factors, and the two nighttime monoterpene ozonolysis factors (R2F4_N and R3F2_N1) correlated well, respectively. However, the contamination factors did not show strong correlation between different ranges, even though undoubtedly from the same source. More about the contamination factors will be discussed in Section 4.1.4. The lower panels in Figure 6 displays the correlations between the first three ranges and the Range Combined, and clearly demonstrates that the results of Range Combined is mainly controlled by high signals from Range 1 and 2. More detailed aspects of the comparison between factors in

different ranges is given in the following sections. The good agreements between factors from different subranges also help to verify the robustness of the solutions.

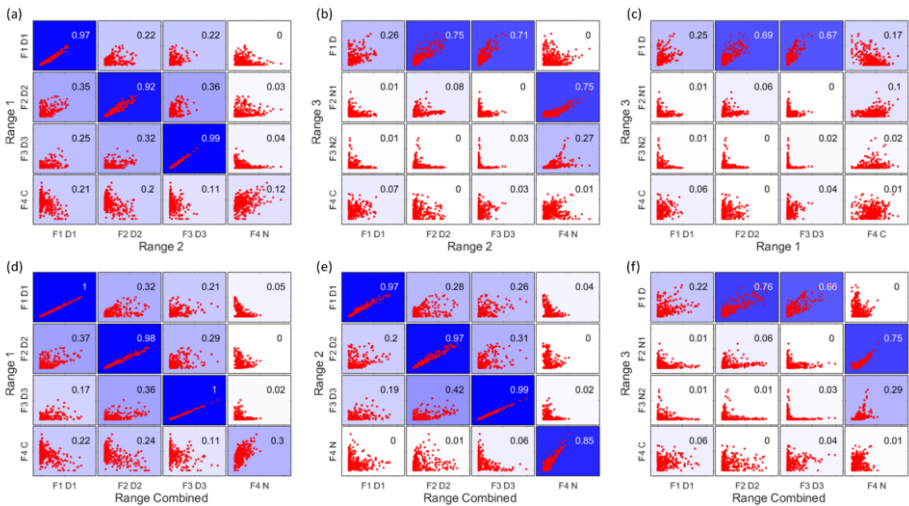


Figure 6 Time series correlations among Range 1, 2, 3 (upper panels a-c), and between the first three ranges and the Range Combined (lower panels d-f). The abbreviations for different factors are the same in Table 1, with F for factor, D for daytime, N for nighttime and C for contamination, e.g. F1D1 for Factor 1 daytime 1. The coefficient of determination, R^2 , is marked in each subplot by a number shown in the right upper corners and by the blue colors, with stronger blue indicating higher R^2 .

Formatted: Font: 11 pt

4.1.2 Daytime factor comparison processes

Formatted: Font: Bold

4.2.1 Factor comparison

Formatted: Font: Bold

As mentioned above, with increasing number of factors, usually more daytime factors will be resolved, reflecting the complicated daytime photochemistry. The three daytime factors between Range 1 and 2 agreed with each other quite well (Figure 6a). However, R1F1_D1 and R2F1_D1 did not show strong correlation with the only daytime factor in Range 3 (R3F1_D), while the other two daytime factors in both Range 1 and 2, i.e. R1F2_D2, R1F3_D3, R2F2_D2, R2F3_D3, correlated well with R3F1_D from Range 3.

The 1st daytime factors from Range 1 and 2, R1F1_D1 and R2F1_D1, were mainly characterized by odd masses 255 Th, 281 Th, 283 Th, 295 Th, 297 Th, 307 Th, 309 Th, 311 Th, 323 Th, 325 Th, 339 Th. The factors are dominated by organonitrates. Organic nitrate formation during daytime is generally associated with the termination of RO₂ radicals by NO. This termination step is mutually

exclusive with the termination of RO₂ with other RO₂, ~~which can lead~~leading to dimer formation. If the NO concentration is the limiting factor for the formation of these factors, the low correlations between the NO-terminated monomer factors, and the dimer factors, is to be expected. In contrast, if the other daytime factors mainly depend on oxidant and monoterpene concentrations, some correlation between those, and the daytime dimer factor, is to be expected, as shown in Figure 6b, c. All the spectral profiles resolved from Range Combined binPMF analysis inevitably contained mass contribution from 510 – 560 Th, even the daytime factor from Range Combined (RCF1_D1) which did not show clear correlation with R3F1_D from Range 3 (Figure 6e).

The 2nd and 3rd daytime factors in Range 1 and 2, R1F2_D2, R1F3_D3, R2F2_D2, R2F3_D3, had high correlations with R3F1_D in Range 3. Daytime factors in Range Combined (RCF2_D2 and RCF3_D3) also showed good correlation with R3F1_D in Range 3. However, if we compare R3F1_D and the mass range of 510 – 560 Th of the daytime factors in Range Combined, just with a quick look, we can readily see the difference. The daytime factor separated in Range 3 (R3F1_D) ~~basically~~ has no obvious markers in the profile. ~~With the increase of factor number (up to ten factors), no clearly new factors were separated in Range 3, but instead the previously separated factors were seen to split into several factors. However, the spectral pattern in R3F1_D is different from that in the mass range of 510 – 560 Th in RCF2_D2. The factorization of Range Combined was mainly controlled by low masses due to their high signals. The signals at high masses were forced to be distributed according to the time series determined by small masses, and as mentioned above, up to ten factors, there would only be more factors fragmented from the previous factor, with similar spectral profiles, but showed different profile pattern with 510 – 560 Th in RCF2_D2 in Range Combined. The factorization of Range Combined was mainly controlled by Range 1 and 2 due to high signals, and the signals in Range 3 are forced to be distributed according to the time series determined by Ranges 1 and 2. Ultimately, this will lead to failure in factor separation for this low-signal range.~~

4.2.2 Daytime dimer formation

Dimers are primarily produced during nighttime, due to NO suppressing RO₂ + RO₂ reactions in daytime (Ehn et al., 2014; Yan et al., 2016). However, in this study, we found one clear daytime factor in Range 3 (R3F1_D, peak at local time 12:00, UTC+2) by sub-range analysis. With high loadings from even masses including 516, 518, 520, 528, 540 Th, this only daytime factor in dimer range correlated very well with two daytime factors in Ranges 1 and 2 (R1F2_D2, R1F3_D3, R2F2_D2, R2F3_D3) (Figure 6b and c). Table 2 include the correlation matrix of all PMF and factors and selected meteorological parameters. Strong correlation between R3F1_D with solar radiation was found, with R = 0.79 (Table 2). This may indicate involvement of OH oxidation in producing this factor.

Formatted: No underline, Font color: Auto

Formatted: Font color: Auto

Formatted: Font: Not Bold

Field Code Changed

Table 2 Correlation between factors and meteorological parameters and gases

	R1F1_D1	R1F1_D2	R1F1_D3	R1F1_C	R2F1_D1	R2F1_D2	R2F1_D3	R2F1_N	R3F1_D	R3F1_N1	R3F1_N2	R3F1_C	R3F1_D1	R3F1_D2	R3F1_D3	R3F1_N
O ₃	0.51	0.59	0.35	-0.18	0.47	0.57	0.36	0.43	0.55	0.33	0.27	0.22	0.49	0.57	0.33	0.34
NO	0.13	-0.01	0.24	-0.03	0.18	-0.02	0.24	-0.22	0.13	-0.19	-0.17	0.03	0.13	0.00	0.26	-0.18
NO _x	-0.05	-0.22	-0.10	0.09	-0.01	-0.23	-0.11	-0.13	-0.16	-0.21	-0.04	0.04	-0.04	-0.22	-0.09	-0.11
RH	-0.46	-0.80	-0.63	0.30	-0.43	-0.82	-0.64	-0.27	-0.78	-0.39	-0.07	-0.07	-0.43	-0.82	-0.60	-0.21
T	0.66	0.72	0.40	-0.24	0.65	0.66	0.41	0.39	0.65	0.30	0.14	0.19	0.66	0.68	0.38	0.24
UVB	0.52	0.63	0.82	-0.40	0.52	0.68	0.84	-0.30	0.79	-0.08	-0.27	0.08	0.49	0.68	0.83	-0.29

As previous studies have shown, dimers greatly facilitate new particle formation (NPF) (Kirkby et al., 2016; Troestl et al., 2016; Lehtipalo et al., 2018), and this daytime dimer factor may represent a source of dimers that would impact the initial stages of NPF in Hyytiälä. Mohr et al. (2017) reported a clear diel pattern of dimers (sum of about 60 dimeric compounds of C₁₆₋₂₀H₁₃₋₃₃O₆₋₉) during NPF events in 2013 in Hyytiälä, with minimum at night and maximum after noon, and estimated these dimers can contribute ~5% of the mass of sub-60 nm particles. The link between the dimers presented in that paper and those reported here will require further studies, as will the proper quantification of the dimer factor identified here.

4.1.3 Nighttime factor comparison processes

4.3.1 Factor comparison

Since high-mass dimers are more likely to form at night due to photochemical production of NO in daytime, which inhibits RO₂ + RO₂ reactions, Range 3 had the highest fraction of nighttime signals of all the sub-ranges. While Range 3 produced two nighttime factors, Ranges 2 and Combined showed one, and Range 1 had no nighttime factor. The difference between the two results also indicates the advantage of analyzing monomers and dimers separately.

The two nighttime factors in Range 3 can be clearly identified as arising from ozonolysis (R3F2_N1) and a mix of ozonolysis and NO₃ oxidation (R3F2_N2) based on the mass spectral profiles, as described above. The organonitrate at 555 Th, C₂₀H₃₁O₁₀NO₃·NO₃⁻, is a typical marker for NO₃ radical initiated monoterpene chemistry (Yan et al., 2016). However, several interesting features become evident when comparing to the results of Range 2 and Combined. Firstly, only one nighttime factor (R2F4_N, RCF4_N) was separated in each of these ranges, and that shows clear resemblance with ozonolysis of monoterpenes as measured in numerous studies, e.g. (Ehn et al., 2012; Ehn et al.,

Field Code Changed

Field Code Changed

Formatted: Font color: Text 1

Formatted: Font: Bold

Field Code Changed

Field Code Changed

2014). Secondly, the high correlation found in Figure 6b between the ozonolysis factors (i.e., R2F4_N, R3F2_N1, RCF4_N), further supports the assignment. However, this factor R2F4_N is the only nighttime factor in the monomer range, suggesting that NO₃ radical chemistry of monoterpenes in Hyytiälä does not form substantial amounts of HOM monomers. The only way for the CI-API-TOF to detect products of monoterpene-NO₃ radical chemistry may thus be through the dimers, where one highly oxygenated RO₂ radical from ozonolysis reacts with a less oxygenated RO₂ radical from NO₃ oxidation.

In the results by Yan et al. (2016) the combined UMR-PMF of monomers and dimers did yield a considerable amount of compounds in the monomer range also for the NO₃ radical chemistry factor. There may be several reasons for this discrepancy. One major cause for differences between the spring dataset of Yan et al. (2016) and the autumn dataset presented here, is that nighttime concentrations of HOM was greatly reduced during our autumn campaign. The cause may have been fairly frequent fog formation during nights, and also the concentration of e.g. ozone decreased nearly to zero during several nights (Zha et al., 2018). It is also possible that the NO₃ radical-related factor by Yan et al. (2016) is probably a mixture of NO₃ and O₃ radical chemistry, while the monomer may thus be attributed to the O₃ part. Alternatively, the different conditions during the two measurement periods, as well as seasonal difference in monoterpene mixtures (Hakola et al., 2012), caused variations in the oxidation pathways.

4.3.2 Dimers initiated by NO₃ radicals

Previous studies show that NO₃ oxidation of α -pinene, the most abundant monoterpene in Hyytiälä (Hakola et al., 2012), produces fairly little SOA mass (yields <4 %), while β -pinene shows yields of up to 53 % (Bonn and Moorgat, 2002; Nah et al., 2016). The NO₃+ β -pinene reaction results in low volatile organic nitrate compounds with carboxylic acid, alcohol, and peroxide functional groups (Fry et al., 2014; Boyd et al., 2015), while NO₃+ α -pinene reaction will typically lose the nitrate functional group and form oxidation products with high vapor pressures (Spittler et al., 2006; Perraud et al., 2010). Most monoterpene-derived HOM, including monomers, are low-volatile (Peräkylä et al., 2020) and thus a low SOA yield indicates a low HOM yield. Thus, while there are to our knowledge no laboratory studies on HOM formation from NO₃ oxidation of α -pinene, a low yield can be expected based on SOA studies.

Field Code Changed

Field Code Changed

Field Code Changed

Field Code Changed

Field Code Changed

Formatted: Font: Bold

Formatted: Font: Bold, Font color: Text 1

Formatted: Tab stops: 1.06", Left

Field Code Changed

Field Code Changed

Field Code Changed

Field Code Changed

Field Code Changed

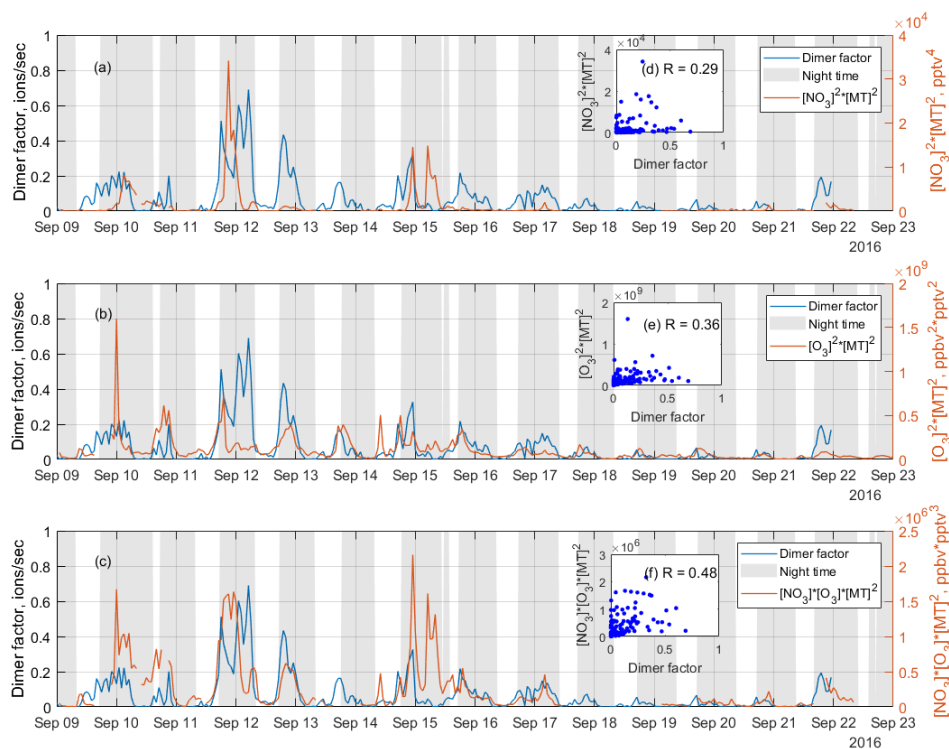


Figure 7 Time series of the NO_3 oxidation dimer factor (blue line), and the product of (a) $[\text{NO}_3]^2 \times [\text{monoterpene}]^2$, (b) $[\text{O}_3]^2 \times [\text{monoterpene}]^2$, and (c) $[\text{NO}_3] \times [\text{O}_3] \times [\text{monoterpene}]^2$, where $[\]$ represents concentration in unit of pptv for NO_3 radicals and monoterpene, ppbv for O_3 , while the scatter plots are shown as inserts, (d), (e), (f), respectively. The scatter plots and correlation coefficients R are only calculated from nighttime data, which is selected based on solar radiation, to eliminate the influence from daytime oxidation processes.

As discussed above, a dimer factor (R3F2 N2) was identified as being a crossover between NO_3 radical initiated and O_3 initiated RO_2 radicals. Figure 7 shows the time series of this factor, as well as the product of $[\text{NO}_3]^2 \times [\text{monoterpene}]^2$, $[\text{O}_3]^2 \times [\text{monoterpene}]^2$, and $[\text{NO}_3] \times [\text{O}_3] \times [\text{monoterpene}]^2$. These products are used to mimic the formation rates of the RO_2 radicals reacting to form the dimers, either from pure NO_3 oxidation (Fig. 7a), pure O_3 oxidation (7b), or the mixed reaction between RO_2 from the two oxidants (7c). The NO_3 concentration was estimated in Liebmann et al. (2018) for the same campaign. Monoterpenes were measured using a proton transfer reaction time of flight mass spectrometer (PTR-TOF-MS). More details on measurement of NO_3 proxy and monoterpene can be found in in Liebmann et al. (2018).

Formatted: Font: 11 pt, No underline, Font color: Auto

Formatted: Line spacing: single

Formatted: Font: 11 pt, Font color: Auto

Formatted: No underline, Font color: Auto

Formatted: Line spacing: 1.5 lines

Formatted: No underline, Font color: Auto

Formatted: No underline, Font color: Auto

Formatted: No underline, Font color: Auto

Formatted: No underline, Font color: Auto

581 As shown in Figure 7, the time series of the dimer factor tracks those of $[\text{NO}_3] \times [\text{monoterpene}]$ and
582 $[\text{O}_3] \times [\text{monoterpene}]$ reasonably well, but shows the highest correlation with the product of $[\text{NO}_3] \times$
583 $[\text{O}_3] \times [\text{monoterpene}]^2$. This further supports this dimer formation as a mixed processes of ozonolysis
584 and NO_3 oxidation. The heterogeneity of the monoterpene emissions in the forest, and the fact that
585 no dimer loss process is included, partly explain the relatively low correlation coefficients. The
586 sampling inlets for PTR-TOF were about 170 m away from the NO_3 reactivity measurement
587 (Liebmann et al., 2018), which in turn was some tens of meters away from the HOM measurements.
588 Thus, this analysis should be considered qualitative only.

Formatted: No underline, Font color: Auto

Formatted: No underline, Font color: Auto

589 The nitrate dimer factor (R3F2 N2) was dominated by the organonitrate at 555 Th, $\text{C}_{20}\text{H}_{31}\text{O}_{10}\text{NO}_3\cdot\text{NO}_3^-$. Liebmann et al. (2018)(Liebmann et al., 2018)However, unlike the pure
590 ozonolysis dimer factor which had a corresponding monomer factor ($R = 0.86$ between factor
591 R2F4 N and R3 F2 N1), this NO_3 -related dimer factor did not have an equivalent monomer factor.
592 This suggests that the NO_3 oxidation of the monoterpene mixture in Hyytiälä does not by itself form
593 much HOM, but in the presence of RO_2 from ozonolysis, the RO_2 from NO_3 oxidation can take part
594 in HOM dimer formation. This further implies that, different from previous knowledge based on
595 single-oxidant experiments in chambers, NO_3 oxidation may have a larger impact on SOA formation
596 in the atmosphere where different oxidants exist concurrently. This highlights the need for future
597 laboratory studies to consider systems with multiple oxidants during monoterpene oxidation
598 experiments, to truly understand the role and contribution of different oxidants, and NO_3 in particular.

Formatted: Don't adjust right indent when grid is defined, Space After: 12 pt, Don't snap to grid

Field Code Changed

Field Code Changed

Formatted: Font color: Red, (Asian) Chinese (PRC)

601 4.4.1.4 Contamination factorFluorinated compounds

602 During the campaign, an automated instrument zeroing every three hours was conducted, by
603 switching a valve to pass the air through a HEPA filter. Each zeroing process lasted for 10 min. While
604 the zeroing successfully removed the low-volatile HOM and H_2SO_4 , the zeroing process also
605 introduced contaminants into the inlet lines, e.g. perfluorinated organic acids from Teflon tubing. The
606 contaminants were primarily different types of perfluorinated organic acids, often off-gassing from
607 e.g. Teflon tubing. For IVOC contaminants, these would be flushed through the inlet, while (E)LVOC
608 would condense onto the inlet walls and not come off. However, SVOC contaminants may stick to
609 the inlet tubing and slowly evaporate back into the sampled air. Each zeroing process lasted for 10
610 min. In the data analysis, we removed all the 10-min zeroing periods, and averaged the data to 1-h
611 time resolution, but contaminants were still identified in all ranges by binPMF. However, the
612 correlation between contamination factors from different ranges is low (Figure 6c).

Formatted: Font: Bold

Formatted: Font: Bold

Formatted: Font: Bold, Font color: Red

Formatted: English (United States)

To future investigate the low factor correlations of the same source, three fluorinated compounds with different volatilities, $(\text{CF}_2)_3\text{CO}_2\text{HF}\cdot\text{NO}_3^-$ (275.9748 Th), $(\text{CF}_2)_5\text{C}_2\text{O}_4\text{H}^-$ (338.9721 Th), and $(\text{CF}_2)_6\text{CO}_2\text{HF}\cdot\text{NO}_3^-$ (425.9653 Th), were examined in fine time resolution, i.e. 1 min. The time series and 3-h cycle of the three fluorinated compounds were shown in Figure S3 and S4 in Supplement. The correlation coefficients dropped greatly ~~when~~ before and after the zero period was removed, from 0.9 to 0.3 for R^2 between 276 Th and 339 Th, and 0.8 to 0.1 between 276 Th and 426 Th (Fig. S5a, b). Similar effect is also found with the 1 h averaged data (Fig. S45c, d). It is evident that the three fluorinated compounds were from the same source (zeroing process), but due to their different volatilities, they were lost at different rates. This, in turn, means that the spectral signature of this source will change as a function of time, at odds with one of the basic assumptions of PMF.

Contamination contributed 10%, 3%, 19% and 4% to Range 1, 2, 3, and Combined, respectively, in the binPMF solutions where the contamination factor was first separated. This also explains why the contamination factor was separated much earlier in Ranges 1 and 3 than in Range 2. However, despite contributing slightly more to Range Combined than to Range 2, the contamination factor was separated when the factor number was increased by one in Range Combined. Here, the difference in volatility of the contaminants in the different sub-ranges may play a role, such that the contaminants in different sub-ranges behave differently. Thus, the behavior of the contamination factor across the combined range is not consistent. Therefore, we examined the zeroing effect with finer time resolution, i.e. 1 min, with three of the largest fluorinated compounds in each range of our mass spectrum, $(\text{CF}_2)_3\text{CO}_2\text{HF}\cdot\text{NO}_3^-$ (275.9748 Th), $(\text{CF}_2)_5\text{C}_2\text{O}_4\text{H}^-$ (338.9721 Th), and $(\text{CF}_2)_6\text{CO}_2\text{HF}\cdot\text{NO}_3^-$ (425.9653 Th). Since the overall signal levels were very low for these compounds, the time series became very noisy with such high time resolution. This made it impossible to perform HR fitting for the data, and instead we summed up the signal from the mass ranges where we expected unperturbed signal from these ions.

The time series with sawtooth pattern of the three fluorinated compounds is shown in Figure S3 in Supplement. From the time series, we selected a period of around three days of the 3-h cycles (25 in total), and in Figure 7 the cycles were aligned and superimposed on top of one another, normalized by the maximum during the zeroing. The normalized signals of the three compounds are shown in light colors, and the mean values shown in bold sold lines. This data includes also the zeroing periods to highlight the effect, but these periods were removed from the data used for our PMF analyses.

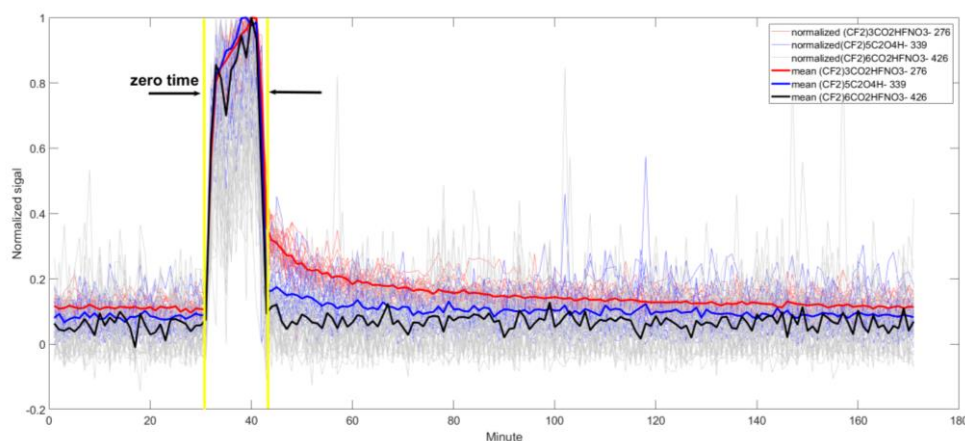


Figure 7 Normalized signals for three fluorinated compounds during a 3-h cycle (180 minutes), with $(\text{CF}_2)_3\text{CO}_2\text{HF}\cdot\text{NO}_3^-$ (275.9748 Th) in red, $(\text{CF}_2)_5\text{C}_2\text{O}_4\text{H}^-$ (338.9721 Th) in blue, and $(\text{CF}_2)_6\text{CO}_2\text{HF}\cdot\text{NO}_3^-$ (425.9653 Th) in black. We selected 25 cycles and normalized all the cycles by their individual maximum. The yellow window shows the zeroing time, for around 10 minutes, which has been removed from the data analysis. Light colors display the individual cycles, and the bold solid colors stand for the average for each compounds.

The signals of the three fluorinated compounds increased by 10 to 20 times during the zeros, due to off-gassing either in the filter or in the tubing in the zeroing setup. Immediately after the zeroing was stopped, signals of all three compounds dropped by about 60-90%, followed by a gradual decay. The decay period coincided with our ambient sampling, and therefore these signals are part of our dataset. It is evident that the three fluorinated compounds were from the same source (zeroing process), but due to their different volatilities, they were lost at different rates. This, in turn, means that the spectral signature of this source will change as a function of time, at odds with one of the basic assumptions of PMF. Panels a and b in Figure S4 displays the temporal correlation with and without zeroing period with 1 min time resolution. The correlation coefficients dropped greatly when the zero period was removed, from 0.9 to 0.3 for R^2 between 276 Th and 339 Th, and 0.8 to 0.1 between 276 Th and 426 Th. Similar effect is also found with the 1 h averaged data (Fig. S4c, d).

The analysis of the is-detailed-analysis-of fluorinated contamination-compounds in our system was here merely used as an example to show that volatility can impact source profiles over time. In this case, the contamination factor was still identified both from the separate sub-ranges and from the combined data set using binPMF. However, the contamination profile in the combined range is now averaged, compared to that from separate ranges: the fractional contributions of contamination

compounds to this profile, vary during the process of each zeroing due to different volatility properties. In Figure S5, contamination factor profiles from Range 3 and Range Combined were compared. It can be clearly seen that the profile of Range Combined is more noisy than that of Range 3, probably due to the varied fractional contributions of contamination compounds to the profile. In ambient data, products from different sources can have undergone atmospheric processing, altering the product distribution. Our aim with this analysis was to highlight the importance of differences in the sink terms due to different volatilities of the products. This may be an important issue for gas phase mass spectrometry analysis, potentially underestimated by many PMF users, as it is likely only a minor issue for aerosol data, for which PMF has been applied much more routinely. If failing to achieve physically meaningful factors using PMF on gas phase mass spectra, our recommendation is to try applying PMF to sub-ranges of the spectrum, where IVOC, SVOC and (E)LVOC could be analyzed separately.

4.5.2 Atmospheric insights

“Based on the new data analysis technique binPMF applied in sub-ranges of mass spectra, we were able to separate two particularly intriguing atmospheric processes, the formation of daytime dimers as well as dimer formation involving NO₃ radicals, which otherwise could not have been identified in our study.

With a diurnal peak around noon time, the daytime dimers identified in this study correlate very well with daytime factors in monomer range. Strong correlation between this factor and solar radiation indicate the potential role of OH oxidation in the formation of daytime dimers. By now, very few studies have reported the observations of daytime dimers. As dimers are shown to be able to take part in new particle formation (NPF) (Kirkby et al., 2016), this daytime dimer may contribute to the early stages of NPF in the boreal forest.

The second process identified in our study is the formation of dimers that are a crossover between NO₃ and O₃ oxidation. Such dimers have been identified before (Yan et al., 2016). However, we were not able to identify corresponding HOM monomer compounds. This finding indicates that while NO₃ oxidation of the monoterpenes in Hyytiälä may not undergo autooxidation to form HOM by themselves, they can contribute to HOM dimers when the NO₃-derived RO₂ react with highly oxygenated RO₂ from other oxidants. Multi-oxidant systems should be taken into consideration in future experimental studies on monoterpene oxidation processes.”

While the previous section discussed several findings with atmospheric implications, we highlight two results below, which are particularly intriguing. We also include the correlation matrix of all PMF and factors and selected meteorological parameters in Table 2.

Formatted: Font color: Auto, (Asian) Chinese (PRC)

Formatted: Font: Bold

Formatted: Font: Bold

Formatted: No underline, Font color: Auto

Formatted: Line spacing: 1.5 lines

Table 2 Correlation between factors and meteorological parameters and gases

	R1F1_D1	R1F1_D2	R1F1_D3	R1F1_C	R2F1_D1	R2F1_D2	R2F1_D3	R2F1_N	R3F1_D	R3F1_N1	R3F1_N2	R3F1_C	R3F1_D1	R3F1_D2	R3F1_D3	R3F1_N
O_3	0.51	0.59	0.35	-0.18	0.47	0.57	0.36	0.43	0.55	0.33	0.27	0.22	0.49	0.57	0.33	0.34
NO	0.13	-0.01	0.24	-0.03	0.18	-0.02	0.24	-0.22	0.13	-0.19	-0.17	0.03	0.13	0.00	0.26	-0.18
NO_x	-0.05	-0.22	-0.10	0.09	-0.01	-0.23	-0.11	-0.13	-0.16	-0.21	-0.04	0.04	-0.04	-0.22	-0.09	-0.11
RH	-0.46	-0.80	-0.63	0.30	-0.43	-0.82	-0.64	-0.27	-0.78	-0.39	-0.07	-0.07	-0.43	-0.82	-0.60	-0.21
T	0.66	0.72	0.40	-0.24	0.65	0.66	0.41	0.39	0.65	0.30	0.14	0.19	0.66	0.68	0.38	0.24
UVB	0.52	0.63	0.82	-0.40	0.52	0.68	0.84	-0.30	0.79	-0.08	-0.27	0.08	0.49	0.68	0.83	-0.29

Formatted: Font: 10 pt

Formatted: English (United States)

Formatted: English (United States)

Formatted: English (United States)

Formatted: English (United States)

Formatted: English (United States)

Formatted: English (United States)

Formatted: English (United States)

4.2.1 Daytime dimer formation

Dimers are primarily produced during nighttime, due to NO suppressing $RO_2 + RO_2$ reactions in daytime (Ehn et al., 2014; Yan et al., 2016). However, in this study, we found one clear daytime factor in Range 3 (R3F1_D, peak at local time 12:00, UTC+2) by sub-range analysis. With high loadings from even masses including 516, 518, 520, 528, 540 Th, this only daytime factor in dimer range correlated very well with two daytime factors in Ranges 1 and 2 (R1F2_D2, R1F3_D3, R2F2_D2, R2F3_D3) (Figure 6b and c). Strong correlation between R3F1_D with solar radiation was found, with $R = 0.79$ (Table 2). This may indicate involvement of OH oxidation in producing this factor.

As previous studies have shown, dimers greatly facilitate new particle formation (NPF) (Kirkby et al., 2016; Troestl et al., 2016; Lehtipalo et al., 2018), and this daytime dimer factor may represent a source of dimers that would impact the initial stages of NPF in Hyytiälä. Mohr et al. (2017) reported a clear diel pattern of dimers (sum of about 60 dimeric compounds of $C_{16-20}H_{13-33}O_{6-9}$) during NPF events in 2013 in Hyytiälä, with minimum at night and maximum after noon, and estimated these dimers can contribute ~5% of the mass of sub-60 nm particles. The link between the dimers presented in that paper and those reported here will require further studies, as will the proper quantification of the dimer factor identified here.

4.2.2 Dimers initiated by NO_3 radicals

Previous studies show that NO_3 oxidation of α -pinene, the most abundant monoterpene in Hyytiälä (Hakola et al., 2012), produces fairly little SOA mass (yields <4 %), while β -pinene shows yields of up to 53 % (Bonn and Moorgat, 2002; Nah et al., 2016). The $NO_3 + \beta$ -pinene reaction results in low volatile organic nitrate compounds with carboxylic acid, alcohol, and peroxide functional groups (Fry et al., 2014; Boyd et al., 2015), while $NO_3 + \alpha$ -pinene reaction will typically lose the nitrate functional group and form oxidation products with high vapor pressures (Spittler et al., 2006; Perraud et al., 2010). Most monoterpene-derived HOM, including monomers, are low-volatile (Peräkylä et al.,

Field Code Changed

Field Code Changed

Field Code Changed

Field Code Changed

Field Code Changed

Field Code Changed

Field Code Changed

Field Code Changed

2020) and thus a low SOA yield indicates a low HOM yield. Thus, while there are to our knowledge no laboratory studies on HOM formation from NO₃ oxidation of α -pinene, a low yield can be expected based on SOA studies.

As discussed in section 4.1.3, a dimer factor (R3F2_N2) was identified as a mix of ozonolysis and NO₃ oxidation processes, dominated by the organonitrate at 555 Th, C₂₀H₃₄O₁₀NO₃⁻NO₃⁻. However, unlike the pure ozonolysis dimer factor which had a corresponding monomer factor (R = 0.86 between factor R2F4_N and R3_F2_N1), this NO₃-related dimer factor did not have an equivalent monomer factor. This suggests that the NO₃ oxidation of the monoterpene mixture in Hyytiälä does not by itself form much HOM, but in the presence of RO₂ from ozonolysis, the RO₂ from NO₃ oxidation can take part in HOM dimer formation. This further implies that, different from previous knowledge based on single oxidant experiments in chambers, NO₃ oxidation may have a larger impact on SOA formation in the atmosphere where different oxidants exist concurrently. This highlights the need for future laboratory studies to consider systems with multiple oxidants during monoterpene oxidation experiments, to truly understand the role and contribution of different oxidants, and NO₃ in particular.

5 Conclusions

The recent development in mass spectrometry, combined with factor analysis such as PMF, has greatly improved our understanding of complicated atmospheric processes and sources. However, one of PMF's basic assumptions is that factor profiles remain constant in time, yet for atmospheric gas-phase species, reactions and sinks may violate this assumption. In this study, we conducted separate binPMF analysis on three different sub-ranges to explore the potential benefits of such an approach for producing more physically meaningful factors.

With binPMF applied on sub-ranges, our study identified daytime dimers, presumably initiated by OH/O₃ with a diurnal peak at around noon, which may contribute to NPF in Hyytiälä. Also, based on the sub-range binPMF analysis, we successfully separated NO₃-related dimers which did not have a corresponding monomer factor. The NO₃-related factor was consistent with earlier observations (Yan et al., 2016), but would not have been identified from this dataset without utilizing the different sub-ranges. In future laboratory experiments, more complex oxidation systems may be useful in order to understand the role of NO₃ oxidation in SOA formation. Apart from these two findings, we also find other benefits by applying binPMF on sub-ranges of the mass spectra.

First, volatility affects the PMF results. Different compounds emitted from the same source showed different temporal trends, likely due to differences in volatilities. This increased the difficulties for PMF to separate this source in the combined data set, and the resolved profile was less accurate than

Formatted: Tab stops: 1.06", Left

Formatted: Subscript

Formatted: Subscript

Formatted: Subscript

that of the sub-ranges. Future studies of gas-phase mass spectra should pay attention to this volatility effect on factor analysis.

Secondly, chemistry or sources contributing to the particular range can be better separated. Only the binPMF analysis on Range 3, where HOM dimers are typically observed, resolved two nighttime factors, characterized by monoterpene oxidation related to NO_3 and O_3 oxidation.

Thirdly, peaks with smaller signal intensities can be correctly assigned. The signal intensities between different parts of the mass spectrum may vary by orders of magnitude. In the combined case, the results were almost completely controlled by the higher signals from smaller masses. The separate analysis on Range 3 allowed the low signals to provide important information. In addition, running binPMF on different separate mass ranges also allows us to compare the factors obtained from the different ranges and help to verify the results.

The recent development in mass spectrometry has greatly improved the detection of atmospheric vapors and their oxidation products. Factor analysis, such as PMF, can reduce dimensionality of the big datasets and extract factors relating to different atmospheric pathways/sources. Optimally, PMF can link laboratory-generated spectra with ambient observations, significantly improving our understanding of complicated atmospheric processes. However, one of PMF's basic assumptions is that factor profiles remain constant in time, yet for atmospheric gas-phase species, varying sources, reactions and sinks may violate this assumption. Some of these variations are likely not addressable in the data analysis stage, but others may be. For example, molecules formed from the same source can have different temporal behaviors due to varying volatilities, and thus condense at different rates. Performing PMF separately with smaller ranges may circumvent this problem. By utilizing the newly presented binPMF approach, more variables can be extracted from a narrow mass range compared to traditional UMR PMF, while preserving more information in the spectrum.

We conducted separate binPMF analysis on three different sub-ranges to explore the potential benefits of such an approach for producing more physically meaningful factors. We utilized ambient data measured by CI-API-TOF in a boreal forest environment, and selected sub-ranges from the mass spectrum that roughly corresponded to regions where we would expect the molecules to have similar volatilities and formation pathways. Selected ranges were Range 1 (250–300 Th), Range 2 (300–350 Th), and Range 3 (510–560 Th). binPMF was separately applied to these ranges, as well as to the combination of all three for comparison.

The different sub-ranges produced some similar and some different factors. First of all, volatility of species indeed affect the PMF results. We could clearly prove the benefit of sub-range binPMF using the contamination factor as an example. We found that different compounds emitted from the same source showed different temporal trends, likely due to differences in volatilities. This increased the

Formatted: Subscript

Formatted: Subscript

difficulties for PMF to separate this source in the combined data set, and the resolved profile was still less accurate than in the analysis for the sub-ranges. We recommend that future studies of gas-phase mass spectra should pay attention to this volatility effect on factor analysis.

Secondly, chemistry or sources contributing to the particular range can be better separated. Only the binPMF analysis on Range 3, where HOM dimers are typically observed, resolved two nighttime factors, characterized by monoterpene oxidation related to NO_3 and O_3 oxidation. The monoterpene ozonolysis factor was separated from both Range 2 and 3, showing very good correlation between the ranges and mutually verifying the results.

Thirdly, peaks with smaller signal intensities can be correctly assigned. The signal intensities between different parts of the mass spectrum may vary by orders of magnitude. In the analysis of the combined range, the results were almost completely controlled by the higher signals from Range 1 and 2. The separate analysis on Range 3 allowed the low signals to provide important information, such as the NO_3 oxidation process. In addition, running binPMF on different separate mass ranges also allows us to compare the factors obtained from the different ranges and help to verify the results.

In addition, daytime dimer formation was identified, presumably initiated by OH/ O_3 with a diurnal peak at around noon, which may contribute to NPF in Hyytiälä. Also, based on the sub-range binPMF analysis, we successfully separated NO_3 -related dimers which did not have an equivalent monomer factor. The NO_3 -related factor was consistent with earlier observations (Yan et al., 2016), but would not have been identified from this dataset without utilizing the different sub-ranges. In future laboratory experiments, more complex oxidation systems may be useful in order to understand the role of NO_3 oxidation in SOA formation.

In summary, we identified several reasons to recommend PMF users to try running their analysis on selected sub-ranges in addition to the whole spectra. Ultimately, the approach should be study-goal dependent. In some cases the researcher wants a quick factor analysis to explore different features of their data, while in others more accurate and quantitative separation of different sources and atmospheric processes are needed. As binPMF and UMR-PMF both require very little data preparation, we expect that it in most cases will be worth the time for the analyst to test how PMF results look for a few selected sub-ranges of their mass spectra.

Data availability. The data used in this study are available from the first author upon request: please contact Yanjun Zhang (yanjun.zhang@helsinki.fi).

Author contributions. ME and YZ designed the study. QZ and MR collected the data; data analysis and manuscript writing were done by YZ. All coauthors discussed the results and commented the manuscript.

Field Code Changed

842 **Competing interests.** The authors declare that they have no conflict of interest

843 **Acknowledgements.** We thank the tofTools team for providing tools for mass spectrometry data
844 analysis. The personnel of the Hyytiälä forestry field station are acknowledged for help during field
845 measurements.

846 **Financial support.** This research was supported by the European Research Council (Grant 638703-
847 COALA), the Academy of Finland (grants 317380 and 320094), and the Vilho, Yrjö and Kalle
848 Väisälä Foundation. K.R.D. acknowledges support by the Swiss National Science postdoc mobility
849 grant P2EZP2_181599.

850

851 Reference

- 852 Äijälä, M., Heikkinen, L., Fröhlich, R., Canonaco, F., Prévôt, A. S. H., Junninen, H., Petäjä, T., Kulmala, M.,
853 Worsnop, D., and Ehn, M.: Resolving anthropogenic aerosol pollution types – deconvolution and
854 exploratory classification of pollution events, *Atmos. Chem. Phys.*, 17, 3165-3197, 10.5194/acp-17-
855 3165-2017, 2017.
- 856 Allan, J. D., Jimenez, J. L., Williams, P. I., Alfarra, M. R., Bower, K. N., Jayne, J. T., Coe, H., and Worsnop,
857 D. R.: Quantitative sampling using an Aerodyne aerosol mass spectrometer 1. Techniques of data
858 interpretation and error analysis, *Journal of Geophysical Research: Atmospheres*, 108, 2003.
- 859 Atkinson, R., Aschmann, S. M., Arey, J., and Shorees, B.: Formation of OH radicals in the gas phase reactions
860 of O₃ with a series of terpenes, 97, 6065-6073, 10.1029/92jd00062, 1992.
- 861 Berndt, T., Mentler, B., Scholz, W., Fischer, L., Herrmann, H., Kulmala, M., and Hansel, A.: Accretion Product
862 Formation from Ozonolysis and OH Radical Reaction of α -Pinene: Mechanistic Insight and the
863 Influence of Isoprene and Ethylene, *Environmental Science & Technology*, 52, 11069-11077,
864 10.1021/acs.est.8b02210, 2018a.
- 865 Berndt, T., Scholz, W., Mentler, B., Fischer, L., Herrmann, H., Kulmala, M., and Hansel, A.: Accretion Product
866 Formation from Self- and Cross-Reactions of RO₂ Radicals in the Atmosphere, *Angewandte Chemie*
867 *International Edition in English* 57, 3820-3824, 10.1002/anie.201710989, 2018b.
- 868 Bertram, T. H., Kimmel, J. R., Crisp, T. A., Ryder, O. S., Yatavelli, R. L. N., Thornton, J. A., Cubison, M. J.,
869 Gonin, M., and Worsnop, D. R.: A field-deployable, chemical ionization time-of-flight mass
870 spectrometer, *Atmospheric Measurement Techniques*, 4, 1471-1479, 10.5194/amt-4-1471-2011, 2011.
- 871 Bianchi, F., Kurtén, T., Riva, M., Mohr, C., Rissanen, M. P., Roldin, P., Berndt, T., Crounse, J. D., Wennberg,
872 P. O., Mentel, T. F., Wildt, J., Junninen, H., Jokinen, T., Kulmala, M., Worsnop, D. R., Thornton, J.
873 A., Donahue, N., Kjaergaard, H. G., and Ehn, M.: Highly Oxygenated Organic Molecules (HOM)
874 from Gas-Phase Autoxidation Involving Peroxy Radicals: A Key Contributor to Atmospheric Aerosol,
875 *Chemical Reviews*, 119, 3472-3509, 10.1021/acs.chemrev.8b00395, 2019.
- 876 Bonn, B., and Moorgat, G. K.: New particle formation during α - and β -pinene oxidation by O₃, OH and NO₃,
877 and the influence of water vapour: particle size distribution studies, *Atmos. Chem. Phys.*, 2, 183-196,
878 10.5194/acp-2-183-2002, 2002.
- 879 Boyd, C. M., Sanchez, J., Xu, L., Eugene, A. J., Nah, T., Tuet, W. Y., Guzman, M. I., and Ng, N. L.: Secondary
880 organic aerosol formation from the β -pinene+NO₃ system: effect of humidity and peroxy radical fate,
881 *Atmos. Chem. Phys.*, 15, 7497-7522, 10.5194/acp-15-7497-2015, 2015.
- 882 Buchholz, A., Lambe, A. T., Ylisirniö, A., Li, Z., Tikkanen, O. P., Faiola, C., Kari, E., Hao, L., Luoma, O.,
883 Huang, W., Mohr, C., Worsnop, D. R., Nizkorodov, S. A., Yli-Juuti, T., Schobesberger, S., and
884 Virtanen, A.: Insights into the O₂-dependent mechanisms controlling the
885 evaporation of α -pinene secondary organic aerosol particles, *Atmos. Chem. Phys.*, 19, 4061-4073,
886 10.5194/acp-19-4061-2019, 2019.
- 887 Canagaratna, M., Jayne, J., Jimenez, J., Allan, J., Alfarra, M., Zhang, Q., Onasch, T., Drewnick, F., Coe, H.,
888 and Middlebrook, A.: Chemical and microphysical characterization of ambient aerosols with the
889 aerodyne aerosol mass spectrometer, *Mass Spectrometry Reviews*, 26, 185-222, 2007.

Field Code Changed

Formatted: Font: (Default) Times New Roman

- Canonaco, F., Crippa, M., Slowik, J., Baltensperger, U., and Prévôt, A.: SoFi, an IGOR-based interface for the efficient use of the generalized multilinear engine (ME-2) for the source apportionment: ME-2 application to aerosol mass spectrometer data, *Atmospheric Measurement Techniques*, 6, 3649, 2013.
- Craven, J. S., Yee, L. D., Ng, N. L., Canagaratna, M. R., Loza, C. L., Schilling, K. A., Yatavelli, R. L. N., Thornton, J. A., Ziemann, P. J., Flagan, R. C., and Seinfeld, J. H.: Analysis of secondary organic aerosol formation and aging using positive matrix factorization of high-resolution aerosol mass spectra: application to the dodecane low-NO_x system, *Atmos. Chem. Phys.*, 12, 11795-11817, 10.5194/acp-12-11795-2012, 2012.
- Crippa, M., Canonaco, F., Lanz, V. A., Äijälä, M., Allan, J. D., Carbone, S., Capes, G., Ceburnis, D., Dall'Osto, M., Day, D. A., DeCarlo, P. F., Ehn, M., Eriksson, A., Freney, E., Hildebrandt Ruiz, L., Hillamo, R., Jimenez, J. L., Junninen, H., Kiendler-Scharr, A., Kortelainen, A. M., Kulmala, M., Laaksonen, A., Mensah, A. A., Mohr, C., Nemitz, E., O'Dowd, C., Ovadnevaite, J., Pandis, S. N., Petäjä, T., Poulain, L., Saarikoski, S., Sellegri, K., Swietlicki, E., Tiitta, P., Worsnop, D. R., Baltensperger, U., and Prévôt, A. S. H.: Organic aerosol components derived from 25 AMS data sets across Europe using a consistent ME-2 based source apportionment approach, *Atmos. Chem. Phys.*, 14, 6159-6176, 10.5194/acp-14-6159-2014, 2014.
- Ehn, M., Kleist, E., Junninen, H., Petäjä, T., Lönn, G., Schobesberger, S., Dal Maso, M., Trimborn, A., Kulmala, M., Worsnop, D. R., Wahner, A., Wildt, J., and Mentel, T. F.: Gas phase formation of extremely oxidized pinene reaction products in chamber and ambient air, *Atmos. Chem. Phys.*, 12, 5113-5127, 10.5194/acp-12-5113-2012, 2012.
- Ehn, M., Thornton, J. A., Kleist, E., Sipila, M., Junninen, H., Pullinen, I., Springer, M., Rubach, F., Tillmann, R., Lee, B., Lopez-Hilfiker, F., Andres, S., Acir, I.-H., Rissanen, M., Jokinen, T., Schobesberger, S., Kangasluoma, J., Kontkanen, J., Nieminen, T., Kurten, T., Nielsen, L. B., Jorgensen, S., Kjaergaard, H. G., Canagaratna, M., Dal Maso, M., Berndt, T., Petaja, T., Wahner, A., Kerminen, V.-M., Kulmala, M., Worsnop, D. R., Wildt, J., and Mentel, T. F.: A large source of low-volatility secondary organic aerosol, *Nature*, 506, 476-479, 10.1038/nature13032, 2014.
- El Haddad, I., D'Anna, B., Temime-Roussel, B., Nicolas, M., Boreave, A., Favez, O., Voisin, D., Sciare, J., George, C., Jaffrezo, J. L., Wortham, H., and Marchand, N.: Towards a better understanding of the origins, chemical composition and aging of oxygenated organic aerosols: case study of a Mediterranean industrialized environment, Marseille, *Atmos. Chem. Phys.*, 13, 7875-7894, 10.5194/acp-13-7875-2013, 2013.
- Fry, J. L., Draper, D. C., Barsanti, K. C., Smith, J. N., Ortega, J., Winkler, P. M., Lawler, M. J., Brown, S. S., Edwards, P. M., Cohen, R. C., and Lee, L.: Secondary Organic Aerosol Formation and Organic Nitrate Yield from NO₃ Oxidation of Biogenic Hydrocarbons, *Environmental Science & Technology*, 48, 11944-11953, 10.1021/es502204x, 2014.
- Guenther, A., Hewitt, C. N., Erickson, D., Fall, R., Geron, C., Graedel, T., Harley, P., Klinger, L., Lerdau, M., McKay, W. A., Pierce, T., Scholes, B., Steinbrecher, R., Tallamraju, R., Taylor, J., and Zimmerman, P.: A GLOBAL-MODEL OF NATURAL VOLATILE ORGANIC-COMPOUND EMISSIONS, *Journal of Geophysical Research-Atmospheres*, 100, 8873-8892, 10.1029/94jd02950, 1995.
- Hakola, H., Tarvainen, V., Bäck, J., Ranta, H., Bonn, B., Rinne, J., and Kulmala, M.: Seasonal variation of mono- and sesquiterpene emission rates of Scots pine, *Biogeosciences*, 3, 93-101, 10.5194/bg-3-93-2006, 2006.
- Hakola, H., Hellén, H., Hemmilä, M., Rinne, J., and Kulmala, M.: In situ measurements of volatile organic compounds in a boreal forest, *Atmos. Chem. Phys.*, 12, 11665-11678, 10.5194/acp-12-11665-2012, 2012.
- Hari, P., and Kulmala, M.: Station for Measuring Ecosystem-Atmosphere Relations (SMEAR II), *Boreal Environment Research*, 10, 315-322, 2005.
- Huang, S., Rahn, K. A., and Arimoto, R.: Testing and optimizing two factor-analysis techniques on aerosol at Narragansett, Rhode Island, *Atmospheric Environment*, 33, 2169-2185, [https://doi.org/10.1016/S1352-2310\(98\)00324-0](https://doi.org/10.1016/S1352-2310(98)00324-0), 1999.
- Huffman, J. A., Docherty, K. S., Aiken, A. C., Cubison, M. J., Ulbrich, I. M., DeCarlo, P. F., Sueper, D., Jayne, J. T., Worsnop, D. R., Ziemann, P. J., and Jimenez, J. L.: Chemically-resolved aerosol volatility measurements from two megacity field studies, *Atmos. Chem. Phys.*, 9, 7161-7182, 10.5194/acp-9-7161-2009, 2009.

Formatted: Font (Default) Times New Roman

Formatted: Font (Default) Times New Roman

- Jokinen, T., Sipilä, M., Junninen, H., Ehn, M., Lönn, G., Hakala, J., Petäjä, T., Mauldin III, R. L., Kulmala, M., and Worsnop, D. R.: Atmospheric sulphuric acid and neutral cluster measurements using CI-API-TOF, *Atmospheric Chemistry and Physics*, 12, 4117-4125, 10.5194/acp-12-4117-2012, 2012.
- Kirkby, J., Duplissy, J., Sengupta, K., Frege, C., Gordon, H., Williamson, C., Heinritzi, M., Simon, M., Yan, C., Almeida, J., Troestl, J., Nieminen, T., Ortega, I. K., Wagner, R., Adamov, A., Amorim, A., Bernhammer, A.-K., Bianchi, F., Breitenlechner, M., Brilke, S., Chen, X., Craven, J., Dias, A., Ehrhart, S., Flagan, R. C., Franchin, A., Fuchs, C., Guida, R., Hakala, J., Hoyle, C. R., Jokinen, T., Junninen, H., Kangasluoma, J., Kim, J., Krapf, M., Kuerten, A., Laaksonen, A., Lehtipalo, K., Makhmutov, V., Mathot, S., Molteni, U., Onnela, A., Peraekylae, O., Piel, F., Petäjä, T., Praplan, A. P., Pringle, K., Rap, A., Richards, N. A. D., Riipinen, I., Rissanen, M. P., Rondo, L., Sarnela, N., Schobesberger, S., Scott, C. E., Seinfeld, J. H., Sipilä, M., Steiner, G., Stozhkov, Y., Stratmann, F., Tome, A., Virtanen, A., Vogel, A. L., Wagner, A. C., Wagner, P. E., Weingartner, E., Wimmer, D., Winkler, P. M., Ye, P., Zhang, X., Hansel, A., Dommen, J., Donahue, N. M., Worsnop, D. R., Baltensperger, U., Kulmala, M., Carslaw, K. S., and Curtius, J.: Ion-induced nucleation of pure biogenic particles, *Nature*, 533, 521-526, 10.1038/nature17953, 2016.
- Kulmala, M., Kontkanen, J., Junninen, H., Lehtipalo, K., Manninen, H. E., Nieminen, T., Petäjä, T., Sipilä, M., Schobesberger, S., Rantala, P., Franchin, A., Jokinen, T., Järvinen, E., Äijälä, M., Kangasluoma, J., Hakala, J., Aalto, P. P., Paasonen, P., Mikkilä, J., Vanhanen, J., Aalto, J., Hakola, H., Makkonen, U., Ruuskanen, T., Mauldin, R. L., Duplissy, J., Vehkamäki, H., Bäck, J., Kortelainen, A., Riipinen, I., Kurtén, T., Johnston, M. V., Smith, J. N., Ehn, M., Mentel, T. F., Lehtinen, K. E. J., Laaksonen, A., Kerminen, V.-M., and Worsnop, D. R.: Direct Observations of Atmospheric Aerosol Nucleation, 339, 943-946, 10.1126/science.1227385 %J Science, 2013.
- Lamarque, J. F., Bond, T. C., Eyring, V., Granier, C., Heil, A., Klimont, Z., Lee, D., Liousse, C., Mieville, A., Owen, B., Schultz, M. G., Shindell, D., Smith, S. J., Stehfest, E., Van Aardenne, J., Cooper, O. R., Kainuma, M., Mahowald, N., McConnell, J. R., Naik, V., Riahi, K., and van Vuuren, D. P.: Historical (1850–2000) gridded anthropogenic and biomass burning emissions of reactive gases and aerosols: methodology and application, *Atmos. Chem. Phys.*, 10, 7017-7039, 10.5194/acp-10-7017-2010, 2010.
- Lee, B. H., Lopez-Hilfiker, F. D., Mohr, C., Kurtén, T., Worsnop, D. R., and Thornton, J. A.: An Iodide-Adduct High-Resolution Time-of-Flight Chemical-Ionization Mass Spectrometer: Application to Atmospheric Inorganic and Organic Compounds, *Environmental Science & Technology*, 48, 6309-6317, 10.1021/es500362a, 2014.
- Lee, B. H., Lopez-Hilfiker, F. D., D'Ambro, E. L., Zhou, P., Boy, M., Petäjä, T., Hao, L., Virtanen, A., and Thornton, J. A.: Semi-volatile and highly oxygenated gaseous and particulate organic compounds observed above a boreal forest canopy, *Atmos. Chem. Phys.*, 18, 11547-11562, 10.5194/acp-18-11547-2018, 2018.
- Lehtipalo, K., Yan, C., Dada, L., Bianchi, F., Xiao, M., Wagner, R., Stolzenburg, D., Ahonen, L. R., Amorim, A., Baccarini, A., Bauer, P. S., Baumgartner, B., Bergen, A., Bernhammer, A.-K., Breitenlechner, M., Brilke, S., Buchholz, A., Mazon, S. B., Chen, D., Chen, X., Dias, A., Dommen, J., Draper, D. C., Duplissy, J., Ehn, M., Finkenzeller, H., Fischer, L., Frege, C., Fuchs, C., Garmash, O., Gordon, H., Hakala, J., He, X., Heikkinen, L., Heinritzi, M., Helm, J. C., Hofbauer, V., Hoyle, C. R., Jokinen, T., Kangasluoma, J., Kerminen, V.-M., Kim, C., Kirkby, J., Kontkanen, J., Kürten, A., Lawler, M. J., Mai, H., Mathot, S., Mauldin, R. L., Molteni, U., Nichman, L., Nie, W., Nieminen, T., Ojdanic, A., Onnela, A., Passananti, M., Petäjä, T., Piel, F., Pospisilova, V., Quéléver, L. L. J., Rissanen, M. P., Rose, C., Sarnela, N., Schallhart, S., Schuchmann, S., Sengupta, K., Simon, M., Sipilä, M., Tauber, C., Tomé, A., Tröstl, J., Väisänen, O., Vogel, A. L., Volkamer, R., Wagner, A. C., Wang, M., Weitz, L., Wimmer, D., Ye, P., Ylisirniö, A., Zha, Q., Carslaw, K. S., Curtius, J., Donahue, N. M., Flagan, R. C., Hansel, A., Riipinen, I., Virtanen, A., Winkler, P. M., Baltensperger, U., Kulmala, M., and Worsnop, D. R.: Multicomponent new particle formation from sulfuric acid, ammonia, and biogenic vapors, 4, eaau5363, 10.1126/sciadv.aau5363 %J Science Advances, 2018.
- Liebmann, J., Karu, E., Sobanski, N., Schuladen, J., Ehn, M., Schallhart, S., Quéléver, L., Hellen, H., Hakola, H., Hoffmann, T., Williams, J., Fischer, H., Lelieveld, J., and Crowley, J. N.: Direct measurement of NO₃ radical reactivity in a boreal forest, *Atmos. Chem. Phys.*, 18, 3799-3815, 10.5194/acp-18-3799-2018, 2018.
- Massoli, P., Stark, H., Canagaratna, M. R., Krechmer, J. E., Xu, L., Ng, N. L., Mauldin, R. L., Yan, C., Kimmel, J., Misztal, P. K., Jimenez, J. L., Jayne, J. T., and Worsnop, D. R.: Ambient Measurements of Highly

- Oxidized Gas-Phase Molecules during the Southern Oxidant and Aerosol Study (SOAS) 2013, ACS Earth and Space Chemistry, 10.1021/acsearthspacechem.8b00028, 2018.
- Mohr, C., Lopez-Hilfiker, F. D., Yli-Juuti, T., Heitto, A., Lutz, A., Hallquist, M., D'Ambro, E. L., Rissanen, M. P., Hao, L., Schobesberger, S., Kulmala, M., Mauldin III, R. L., Makkonen, U., Sipilä, M., Petäjä, T., and Thornton, J. A.: Ambient observations of dimers from terpene oxidation in the gas phase: Implications for new particle formation and growth, 44, 2958-2966, 10.1002/2017gl072718, 2017.
- Nah, T., Sanchez, J., Boyd, C. M., and Ng, N. L.: Photochemical Aging of α -pinene and β -pinene Secondary Organic Aerosol formed from Nitrate Radical Oxidation, Environmental Science & Technology, 50, 222-231, 10.1021/acs.est.5b04594, 2016.
- Orlando, J. J., and Tyndall, G. S.: Laboratory studies of organic peroxy radical chemistry: an overview with emphasis on recent issues of atmospheric significance, J Chemical Society Reviews, 41, 6294-6317, 2012.
- Paatero, P., and Tapper, U.: Positive matrix factorization: A non - negative factor model with optimal utilization of error estimates of data values, Environmetrics, 5, 111-126, 1994.
- Paatero, P.: Least squares formulation of robust non-negative factor analysis, Chemometrics and Intelligent Laboratory Systems, 37, 23-35, [https://doi.org/10.1016/S0169-7439\(96\)00044-5](https://doi.org/10.1016/S0169-7439(96)00044-5), 1997.
- Paatero, P.: The Multilinear Engine—A Table-Driven, Least Squares Program for Solving Multilinear Problems, Including the n-Way Parallel Factor Analysis Model, Journal of Computational and Graphical Statistics, 8, 854-888, 10.1080/10618600.1999.10474853, 1999.
- Paciga, A., Karnezi, E., Kostenidou, E., Hildebrandt, L., Psichoudaki, M., Engelhart, G. J., Lee, B. H., Crippa, M., Prévôt, A. S. H., Baltensperger, U., and Pandis, S. N.: Volatility of organic aerosol and its components in the megacity of Paris, Atmos. Chem. Phys., 16, 2013-2023, 10.5194/acp-16-2013-2016, 2016.
- Paulson, S. E., and Orlando, J. J.: The reactions of ozone with alkenes: An important source of HOx in the boundary layer, 23, 3727-3730, 10.1029/96gl03477, 1996.
- Peräkylä, O., Riva, M., Heikkinen, L., Quéléver, L., Roldin, P., and Ehn, M.: Experimental investigation into the volatilities of highly oxygenated organic molecules (HOM), Atmospheric Chemistry and Physics, 20, 649-669, 10.5194/acp-2019-620, 2020.
- Perraud, V., Bruns, E. A., Ezell, M. J., Johnson, S. N., Greaves, J., and Finlayson-Pitts, B. J.: Identification of Organic Nitrates in the NO₃ Radical Initiated Oxidation of α -Pinene by Atmospheric Pressure Chemical Ionization Mass Spectrometry, Environmental Science & Technology, 44, 5887-5893, 10.1021/es1005658, 2010.
- Polissar, A. V., Hopke, P. K., Paatero, P., Malm, W. C., and Sisler, J. F.: Atmospheric aerosol over Alaska: 2. Elemental composition and sources, Journal of Geophysical Research: Atmospheres, 103, 19045-19057, 1998.
- Pope III, C. A., Ezzati, M., and Dockery, D. W.: Fine-particulate air pollution and life expectancy in the United States, New England Journal of Medicine, 360, 376-386, 2009.
- Riva, M., Rantala, P., Krechmer, J. E., Peräkylä, O., Zhang, Y., Heikkinen, L., Garmash, O., Yan, C., Kulmala, M., Worsnop, D., and Ehn, M.: Evaluating the performance of five different chemical ionization techniques for detecting gaseous oxygenated organic species, Atmospheric Measurement Techniques, 12, 2403-2421, 10.5194/amt-12-2403-2019, 2019.
- Sekimoto, K., Koss, A. R., Gilman, J. B., Selimovic, V., Coggon, M. M., Zarzana, K. J., Yuan, B., Lerner, B. M., Brown, S. S., Warneke, C., Yokelson, R. J., Roberts, J. M., and de Gouw, J.: High- and low-temperature pyrolysis profiles describe volatile organic compound emissions from western US wildfire fuels, Atmos. Chem. Phys., 18, 9263-9281, 10.5194/acp-18-9263-2018, 2018.
- Shiraiwa, M., Ueda, K., Pozzer, A., Lammel, G., Kampf, C. J., Fushimi, A., Enami, S., Arangio, A. M., Fröhlich-Nowoisky, J., Fujitani, Y., Furuyama, A., Lakey, P. S. J., Lelieveld, J., Lucas, K., Morino, Y., Pöschl, U., Takahama, S., Takami, A., Tong, H., Weber, B., Yoshino, A., and Sato, K.: Aerosol Health Effects from Molecular to Global Scales, Environmental Science & Technology, 51, 13545-13567, 10.1021/acs.est.7b04417, 2017.
- Song, Y., Shao, M., Liu, Y., Lu, S., Kuster, W., Goldan, P., and Xie, S.: Source apportionment of ambient volatile organic compounds in Beijing, Environmental science & technology, 41, 4348-4353, 2007.
- Spittler, M., Barnes, I., Bejan, I., Brockmann, K. J., Benter, T., and Wirtz, K.: Reactions of NO₃ radicals with limonene and α -pinene: Product and SOA formation, Atmospheric Environment, 40, 116-127, <https://doi.org/10.1016/j.atmosenv.2005.09.093>, 2006.

Formatted: Font: (Default) Times New Roman

Formatted: Font: (Default) Times New Roman

Formatted: Font: (Default) Times New Roman

Formatted: Font: (Default) Times New Roman

- Stocker, T., Qin, D., Plattner, G., Tignor, M., Allen, S., Boschung, J., Nauels, A., Xia, Y., Bex, V., and Midgley, P.: IPCC, 2013: Climate Change 2013: The Physical Science Basis. Contribution of Working Group I to the Fifth Assessment Report of the Intergovernmental Panel on Climate Change, 1535 pp, in, Cambridge Univ. Press, Cambridge, UK, and New York, 2013.
- Troestl, J., Chuang, W. K., Gordon, H., Heinritzi, M., Yan, C., Molteni, U., Ahlm, L., Frege, C., Bianchi, F., Wagner, R., Simon, M., Lehtipalo, K., Williamson, C., Craven, J. S., Duplissy, J., Adamov, A., Almeida, J., Bernhammer, A.-K., Breitenlechner, M., Brilke, S., Dias, A., Ehrhart, S., Flagan, R. C., Franchin, A., Fuchs, C., Guida, R., Gysel, M., Hansel, A., Hoyle, C. R., Jokinen, T., Junninen, H., Kangasluoma, J., Keskinen, H., Kim, J., Krapf, M., Kuerten, A., Laaksonen, A., Lawler, M., Leiminger, M., Mathot, S., Moehler, O., Nieminen, T., Onnela, A., Petäejae, T., Piel, F. M., Miettinen, P., Rissanen, M. P., Rondo, L., Sarnela, N., Schobesberger, S., Sengupta, K., Sipila, M., Smith, J. N., Steiner, G., Tome, A., Virtanen, A., Wagner, A. C., Weingartner, E., Wimmer, D., Winkler, P. M., Ye, P., Carslaw, K. S., Curtius, J., Dommen, J., Kirkby, J., Kulmala, M., Riipinen, I., Worsnop, D. R., Donahue, N. M., and Baltensperger, U.: The role of low-volatility organic compounds in initial particle growth in the atmosphere, *Nature*, 533, 527-531, 10.1038/nature18271, 2016.
- Ulbrich, I. M., Canagaratna, M. R., Zhang, Q., Worsnop, D. R., and Jimenez, J. L.: Interpretation of organic components from Positive Matrix Factorization of aerosol mass spectrometric data, *Atmos. Chem. Phys.*, 9, 2891-2918, 10.5194/acp-9-2891-2009, 2009.
- Yan, C., Nie, W., Aijala, M., Rissanen, M. P., Canagaratna, M. R., Massoli, P., Junninen, H., Jokinen, T., Sarnela, N., Hame, S. A. K., Schobesberger, S., Canonaco, F., Yao, L., Prevot, A. S. H., Petaja, T., Kulmala, M., Sipila, M., Worsnop, D. R., and Ehn, M.: Source characterization of highly oxidized multifunctional compounds in a boreal forest environment using positive matrix factorization, *Atmospheric Chemistry and Physics*, 16, 12715-12731, 10.5194/acp-16-12715-2016, 2016.
- Zha, Q., Yan, C., Junninen, H., Riva, M., Sarnela, N., Aalto, J., Quéléver, L., Schallhart, S., Dada, L., Heikkinen, L., Peräkylä, O., Zou, J., Rose, C., Wang, Y., Mammarella, I., Katul, G., Vesala, T., Worsnop, D. R., Kulmala, M., Petäjä, T., Bianchi, F., and Ehn, M.: Vertical characterization of highly oxygenated molecules (HOMs) below and above a boreal forest canopy, *Atmos. Chem. Phys.*, 18, 17437-17450, 10.5194/acp-18-17437-2018, 2018.
- Zhang, Q., Jimenez, J. L., Canagaratna, M. R., Ulbrich, I. M., Ng, N. L., Worsnop, D. R., and Sun, Y.: Understanding atmospheric organic aerosols via factor analysis of aerosol mass spectrometry: a review, *Analytical and Bioanalytical Chemistry*, 401, 3045-3067, 10.1007/s00216-011-5355-y, 2011.
- Zhang, Y., Lin, Y., Cai, J., Liu, Y., Hong, L., Qin, M., Zhao, Y., Ma, J., Wang, X., and Zhu, T.: Atmospheric PAHs in North China: spatial distribution and sources, *Science of the Total Environment*, 565, 994-1000, 2016.
- Zhang, Y., Cai, J., Wang, S., He, K., and Zheng, M.: Review of receptor-based source apportionment research of fine particulate matter and its challenges in China, *Science of the Total Environment*, 586, 917-929, 2017.
- Zhang, Y., Peräkylä, O., Yan, C., Heikkinen, L., Äijälä, M., Daellenbach, K. R., Zha, Q., Riva, M., Garmash, O., Junninen, H., Paatero, P., Worsnop, D., and Ehn, M.: A novel approach for simple statistical analysis of high-resolution mass spectra, *Atmospheric Measurement Techniques*, 12, 3761-3776, 10.5194/amt-12-3761-2019, 2019.

Formatted: Finnish